

RESEARCH

Open Access



# Spatial dissimilarity of zooplankton and hydrodynamic conditions in a Patagonian channel used intensely by aquaculture: the influence of a geomorphological constriction

Eduardo Hernández-Miranda<sup>1,2\*</sup> , Ignacio Betancourt<sup>3</sup>, Marcus Sobarzo<sup>1,4</sup>, Odette Vergara<sup>1</sup>, Claudio Iturra<sup>5</sup> and Renato A. Quiñones<sup>1,4</sup>

## Abstract

**Background:** Marine aquaculture is a very important economic and food production activity in Patagonian channels. The biophysical mechanisms through which farms interact with surrounding areas is poorly understood. A better understanding of the relationship between zooplankton distribution, hydrodynamics and aquaculture farms in Patagonian channels can contribute to the environmental sustainability of this activity.

**Methods:** The study was conducted in winter in the Caucahué Channel (Chiloé Island, southern Chile), which is composed of two asymmetric northern and southern sections separated by a geomorphological constriction (a narrows) and hosts 55 aquaculture farms. Intensive zooplankton and water column sampling (time scale: 12 h) was carried out, together with current measurements as a background of the channel hydrodynamics (time scale: 30 days).

**Results:** Spatial dissimilarities in composition and abundances of zooplankton communities and in water column variables were identified between the two sections of the channel in this short-term time scale. In the southern section we found higher abundances of holo- and meroplankton and higher species richness. No differences in zooplankton community were found between sampling sites near and far from aquaculture farms. Southward asymmetrical residual flow and semidiurnal tidal excursion were verified in the central part of the channel during two tidal fortnightly time periods.

**Conclusions:** (i) Clear dissimilarity in zooplankton composition were found between the two sections of Caucahué Channel in the time scale studied; and (ii) Quemchi geomorphological constriction and the asymmetrical southward residual flow could act as a physical barrier favoring the spatial dissimilarities found in biotic and abiotic variables between the two sections of the channel.

**Keywords:** Aquaculture zoning, Coastal circulation, Plankton transport, Mussel farms, Salmon farms

## Background

Marine aquaculture is one of the most important economic activities worldwide [1]. World aquaculture exceeds 73 million tons, with an estimated first-sale value of US\$ 160.2 billion [2]. Chile is a major

\*Correspondence: [ehernandez@ucsc.cl](mailto:ehernandez@ucsc.cl)

<sup>1</sup> Interdisciplinary Center for Aquaculture Research (INCAR), Universidad de Concepción, Casilla 160-C, Concepción, Chile  
Full list of author information is available at the end of the article



© The Author(s) 2022. **Open Access** This article is licensed under a Creative Commons Attribution 4.0 International License, which permits use, sharing, adaptation, distribution and reproduction in any medium or format, as long as you give appropriate credit to the original author(s) and the source, provide a link to the Creative Commons licence, and indicate if changes were made. The images or other third party material in this article are included in the article's Creative Commons licence, unless indicated otherwise in a credit line to the material. If material is not included in the article's Creative Commons licence and your intended use is not permitted by statutory regulation or exceeds the permitted use, you will need to obtain permission directly from the copyright holder. To view a copy of this licence, visit <http://creativecommons.org/licenses/by/4.0/>.

contributor to aquaculture products, mainly salmon and bivalve mussels, with a total of 1,266,100 tons in 2018 [2]. Most of this industry (86% of salmon production and 99% of mussel production) is located in the channels, bays and fjords of the inner sea of Chiloé, between Puerto Montt (41°28'S; 72°57'W) and Boca del Guafo (43°37'S; 73°57'W) [3–6], with a significant impact on local and international markets [7, 8]. There is currently growing interest in acquiring a better understanding of the physical processes and ecological mechanisms through which aquaculture farms interact with parasite outbreaks, spread of diseases and HABs, particularly in the context of the expected changes in Patagonian ecosystems produced by global climate change [9–13]. For instance, it is not clear how to increase production while maintaining a proper distance between farms to reduce the spread of contagious viral diseases (e.g. ISA), bacteria (e.g. *Piscirickettsia salmonis*), and ectoparasites (e.g. *Caligus rogercreseeyi*) [6, 14–18]. After a strong outbreak of the ISA virus in 2007, in 2009 the Chilean government established Aquaculture Management Areas (AMA), also referred to as neighborhoods (see [6] for a review and <http://mapas.intesal.cl> for online assignment of AMAs). Each AMA contains a group of concessions for specific areas, and each farm within the group concession area is licensed. Since AMAs are in close proximity, the Chilean authorities created in 2012 several Macrozones for the specific purpose of containing disease dissemination (see <https://geoportal.subpesc.cl/> for Macrozone assignments). Each Macrozone contains several AMAs, and a minimum distance of 5 nm among them is applied as a preventive measure to stop the spread of diseases [19]. Nevertheless, there is insufficient information about how farms, AMAs and Macrozones interact. Indeed, there is scarce information about how coastal currents connect areas and farms and if residual flows are forced by wind friction, freshwater input or non-linear processes [20]. The influence of residual flows in transporting pathogens, parasites and other planktonic organisms has also not been well documented. Knowledge of local biophysical mechanisms in the AMAs and farms (i.e. relationships between advective transport processes and biological spatial patterns in the water column) has been limited to specific studies of parasites like *C. rogercreseeyi* or to the dispersion of pellets (e.g. [16, 21]).

It is widely known that environmental stressors can alter the structural and functional biodiversity of aquatic ecosystems. The community structure in a particular area can be used as an indicator of local ecological conditions and environmental health [22]. Benthic

macrofauna are frequently used to construct indicators for marine ecosystems because these organisms are relatively sedentary, have relatively long life-spans, consist of different species with different tolerances to stress and have an important biogeochemical and ecological role (e.g. [23–26]). Plankton communities are less used to construct indicators due to their dependence on currents, high degree of spatial heterogeneity, high temporal variability and difficulty in finding recognizable patterns [27–29]. However, plankton indicators are recognized as valuable tools to capture the condition of the environment, as early warning signals and as barometers of long-term trends (e.g. [28, 30–32]). Plankton communities are generally composed of larval stages of vertebrates and invertebrates that are transient in this environment (meroplankton) and organisms that remain throughout their entire lifecycle in the water column, like copepods (holoplankton). The spatial and temporal variability of abundance and composition of holo- and meroplankton species are strongly dependent on local environmental conditions [33]. Knowledge of the spatial distribution of zooplankton communities, their dissimilarities and the environmental conditions of the water column, along with advective transport mechanisms in a determined area, can be a quantitative tool to characterize coastal zones (e.g. Macrozones or AMAs).

The aim of this study was to assess the interaction between zooplankton distribution and hydrodynamics in Caucahué Channel, which is an area intensely used by aquaculture activities. Thus we (i) characterize the zooplankton community distribution, water column characteristics and their relationship during a short time period (hours), (ii) characterize the hydrodynamics of the channel during two fortnightly tidal cycles, and (iii) integrate information about the spatial distribution of the zooplankton community and environmental variables in neap and spring tidal cycles.

## Methods

### Study area

The Caucahué Channel separates Caucahué Island from Chiloé Island in southern Chile (Fig. 1). The channel comprises two asymmetrical sections. The northern section is shorter (7.5 km), with depths shallower than 50 m except near the channel mouth. The southern section is 11.5 km long and deeper, reaching 100 m in some areas. Both sections are connected near Quemchi (42°08'36"S; 73°28'27"W) by a narrow, which is the narrowest (0.8 km) and shallowest (< 45 m) area of the channel (hereafter referred to as

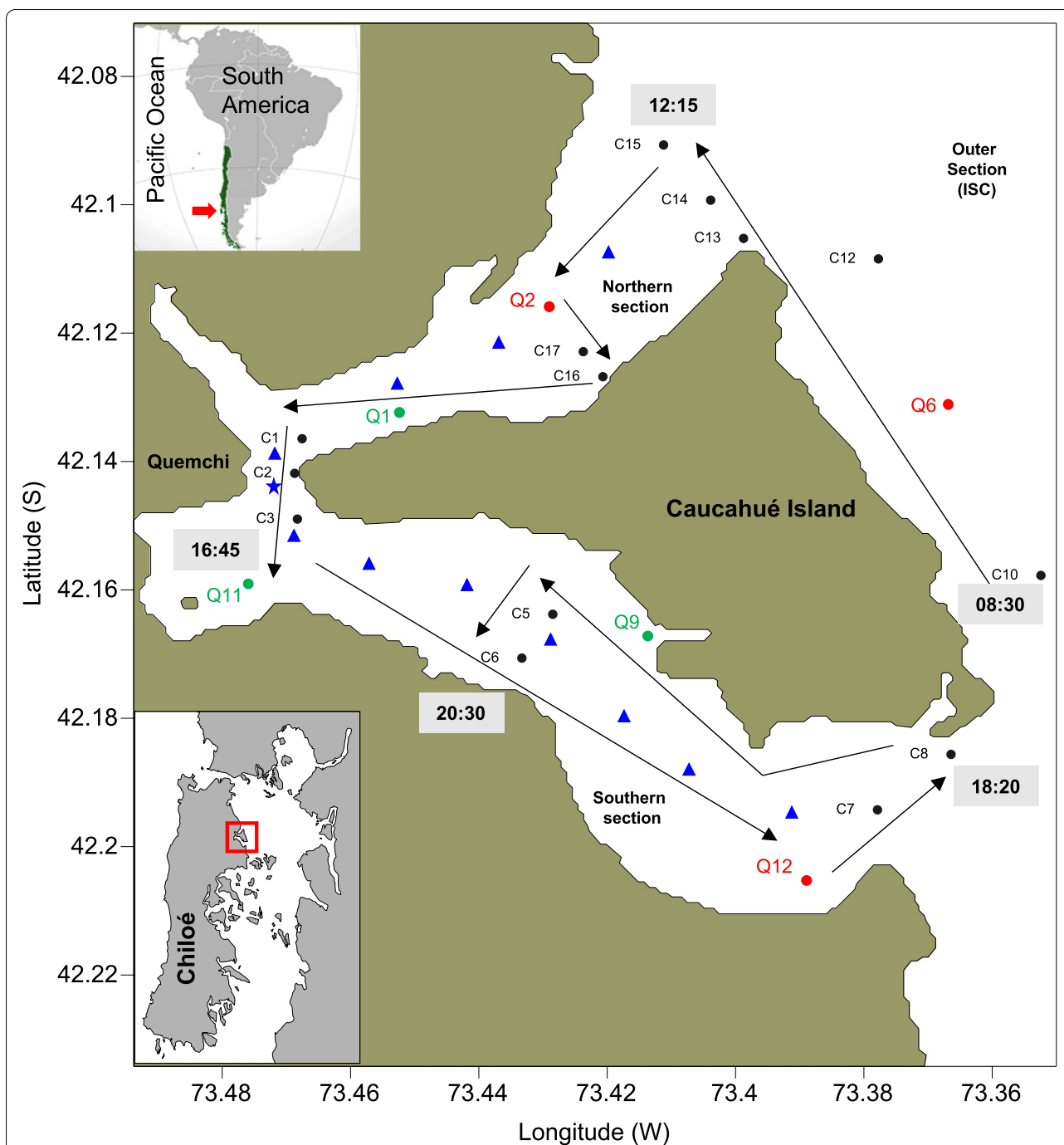


**Fig. 1** The Caucahué Channel. Sampling sites (circles), sampling track (black arrows) and approximate time of zooplankton sampling on June 19. Q sites are near aquaculture centers (green = mytilids, red = salmonids) and C sites are far from aquaculture centers. The zooplankton sampling track begins at site C10 (08:30 h) and ends at site C6 (20:30 h). Blue triangles indicate CTDO sampling sites on June 30. The blue star indicates the ADCP monitoring site

the Quemchi constriction). The cross-sectional area of this constriction (0.017 km<sup>2</sup>) is approximately 10 to 20 times narrower than the southern mouth (0.21

km<sup>2</sup>) and northern mouth (0.38 km<sup>2</sup>) [20]. The Caucahué Channel includes 37 mussel farms, 13 salmon farms and five seaweed farms, of which only a third are

simultaneously active (<https://geoportal.subpesca.cl/>). Caucahué Channel is defined as a single AMA (number 7) and part of sanitary Macrozone 4.

The influence of the semidiurnal tidal excursion and asymmetrical residual flow on the spatial connection among aquaculture farms in this channel was investigated by Sobarzo et al. [20]. The tidal oscillatory component explained 60–80% of the variance of the total current. The estimated southward residual flow was 1.9–2.6 km d<sup>-1</sup> [20]. The Quemchi constriction may act as a natural physical barrier to northward transport. If true, the semidiurnal tidal excursion (short-range connection) in the Caucahué Channel would determine particle/plankton spatial distribution in each channel section on a temporal scale of hours. In contrast, the asymmetrical residual flow (large-range connection) would favor unidirectional transport from the northern to the southern section of the channel in periods longer than seven days [20].

#### Zooplankton and water sampling

To evaluate spatial distribution of the zooplankton community, samples were collected in 20 sites in a period of 12 h (between 8:30 am and 8:30 pm), on June 19, 2014, covering the northern and southern sections of the channel, the adjacent area in the inner sea of Chiloé and the Quemchi constriction. Six sites (Q<sub>i</sub>, See Fig. 1) were located near aquaculture farms (5–50 m from the limits of the farms) and 14 sites (C<sub>i</sub>, See Fig. 1) were located far from active aquaculture farms (500 to 3000 m from the limits of the farms). Zooplankton samples were collected from the surface stratum (0.1 to 0.2 m depth) and the deeper stratum of the water column (10 to 15 m depth). The surface stratum was sampled with an epineuston net 1 m wide and 30 cm high, with a 300- $\mu$ m mesh. The deeper stratum was sampled with a bongo net 0.6 m wide with a 300- $\mu$ m mesh. The nets incorporated flow meters (General Oceanics) to standardize the number of individuals captured in each sample to ind 100 m<sup>-3</sup>. The samples of both strata were taken at the same time (towing time = 5 min) in a small fishing boat. The samples were stored in 95% alcohol for subsequent identification in the laboratory. The samples were analyzed in the laboratory under a stereomicroscope to identify all taxa to the lowest possible taxonomic level of resolution. A zooplankton database was constructed for the abundance of species from the two depth strata. The average abundance of the catch from the two cod ends of the bongo net were used for analysis of the deeper stratum. In the surface stratum, the abundance values at each sampling site correspond to one cod end.

To characterize environmental conditions in each site where zooplankton samples were collected (*i.e.* June 19, 2014), discrete water samples were obtained with a Niskin bottle from the surface (0–0.2 m) and subsurface layers (10–15 m). Temperature (°C), salinity, total dissolved solids (g L<sup>-1</sup>), pH, redox potential (mV) and dissolved oxygen (mL L<sup>-1</sup>) of both layers were recorded with a YSI 556MDS multi-probe system. Complementary vertical profiles of temperature (°C), salinity, density (kg m<sup>-3</sup>), and dissolved oxygen (mL L<sup>-1</sup>) in each sampling site were obtained using a CTDO SAIV A/S, model SD204. Other measurements of temperature (°C), salinity, density (kg m<sup>-3</sup>), and dissolved oxygen (mL L<sup>-1</sup>) were made along the entire channel with a CTDO Sea-Bird Scientific SBE 19 V2 plus on June 30, 2014, between 9:24 h and 12:09 h during ebb tide (See Fig. 1).

Between June 17 and 20, 2014, discrete water samples were obtained between 2 and 50 m depth using a Niskin bottle to determine chlorophyll-*a* (Chl-*a*) and phaeopigment (Feop) concentrations. Four sites (C12, C15, Q2, C1) were sampled in the northern section and three (C3, Q9 and C7) in the southern (Fig. 1). In each stratum 0.5 L of seawater was filtered using glass fiber filters (Wattman GF/F; nominal pore size = 0.7  $\mu$ m) previously muffled at 450 °C for 5 h. Each sample was stored in aluminum pouches at -20 °C until analysis in the laboratory. Chl-*a* and Feop were determined using the method described by Holm-Hansen and Riemann [34]. Pigment extractions were done in the dark. Each thawed filter was inserted into a glass tube with 10 mL acetone (90%) and kept for 24 h at -20 °C. Then the samples were kept for 2–3 h at ambient temperature and homogenized. One ml was extracted and the fluorescence determined with a Turner Designs (Model Trilogy 7200 series®) fluorometer. Then 4 to 5 drops of HCl 5% were added and stirred. The phaeopigment reading was conducted after 1 min. The readings were converted to mg m<sup>-3</sup> of Chl-*a* and Pheop.

#### Hydrodynamic observations

Currents were measured using a 614-kHz ADCP (Work Horse) moored at 45 m depth. The ADCP recorded marine currents every 10 min from June 6 to July 5, 2014, with a vertical resolution of one meter. The ADCP was deployed near the Quemchi constriction (Fig. 1). Due to the orientation of the coastline in the Quemchi constriction, currents were decomposed into their north–south (*y*) and east–west (*x*) axes. Harmonic analysis using the T-Tide Program allows quantifying the contribution of the main tidal constituents

to the total current [35]. Subsequently, de-tided currents were filtered to suppress high-frequency fluctuations using a symmetrical low-pass filter (half power at 0.6 cpd). The mean residual flow and the variance of subtidal circulation in the Quemchi constriction were estimated using filtered currents. Based on the north–south component of the total current, we calculated the number of hours and average speed associated with the positive (flood) and negative (ebb) values, considering the neap and spring tides. Also, the ratio between the residual advective distance ( $L_{adv}$ ) and the tidal excursion ( $L_{exc}$ ) was calculated to estimate the transport in ebb and flood conditions and during neap and spring tides. A detailed description of the methodology can be found in Sobarzo et al. [20].

### Statistical analysis

The first exploratory analysis of community zooplankton abundance datasets was conducted comparing the samples obtained at the surface and deeper strata. The initial homoscedasticity analysis indicated heterogeneity between the zooplankton communities of the two depth strata. Accordingly, subsequent analyses were conducted by stratum separately, identifying the presence of natural groups (without a priori spatial assignment), which were compared visually and statistically. The first step in analyzing the zooplankton from each stratum was to select a measure of dissimilarity. The Jaccard dissimilarity measure was calculated with zooplankton abundance data converted to presence-absence, while the Bray–Curtis measure was calculated without transformation and with fourth-root transformed data. Different measures of dissimilarity and transformation were employed because they contribute to different interpretations of the community under study [36–38]. Non-metric multidimensional scaling analyses (nMDS) were generated with the dissimilarity measures to identify groups without prior spatial assignment. Cluster analyses using hierarchical and non-hierarchical methods ( $K$ -means) were applied to confirm the observed groups objectively, considering 2, 3, 4 and 5 independent groups for each cluster. The hierarchical method that presented the highest cophenetic correlation was chosen for each measurement of dissimilarity [39]. The mean silhouette coefficient was used to assess the quality of the clusters [40], selecting the grouping that yielded the highest value to measure dissimilarity and transformation. A minimum silhouette value of 0.25 was employed to decide that a grouping of elements (*i.e.* sampling sites) is not merely random [41]. The strongest grouping was selected for each measure of dissimilarity and for each stratum.

The second step consisted of determining whether the identified groups are significantly different in their multivariate beta diversity [37]. A non-parametric MANOVA means test was applied for this purpose using PERMANOVA [36, 37]. The analysis was applied to compare differences between the strongest groupings in each dissimilarity measure for both strata. The homoscedasticity in the multivariate dispersion of the groups was the first to be confirmed. Finally, a consensus dendrogram was generated with the data from the sampling sites assigned to significantly dissimilar groupings, with the objective of identifying potential outlier sites for each stratum. Complementary to this and with the aim of determining whether there are significant differences in multivariate beta diversity between sites close to and far from aquaculture farms (See Fig. 1), similar homoscedasticity tests and multivariate means comparisons were made for each dissimilarity measure. The analyses were done with the public domain software R and the special Vegan package.

The relationship between zooplankton composition/abundance and environmental variables measured with the YSI 556MDS multi-probe system were analyzed separately for the surface and deeper stratum. Zooplankton groupings were estimated and statistically validated by a distance-based linear DistLM model [42], which analyzes the influence of the set of environmental variables on the dissimilarities found among zooplankton communities (*i.e.* sites). The best models were selected for each stratum, dissimilarity measure and data transformation using the Akaike information criterion (AICc). Graphic output of the fitted model in a multi-dimensional space was visualized using distance-based redundancy analysis (dbRDA). Finally, Similarity Percentage Analysis (SIMPER) was used to identify the main taxa/species of mero- and holoplankton that contribute to community dissimilarity for each stratum and among sampling sites. PRIMER v7 and PERMANOVA+ were used for these analyses [38, 42].

## Results

### Multivariate diversity and environmental variables

Figure 2 shows the nMDS analysis of zooplankton incorporating the surface and the deeper strata. For the different dissimilarity measures (Bray–Curtis without transformation, transformed to fourth root and Jaccard converted to presence-absence), there was a higher degree of homogeneity in the zooplankton community in the deeper layer than in the surface layer (*i.e.* less dispersion among sampling sites

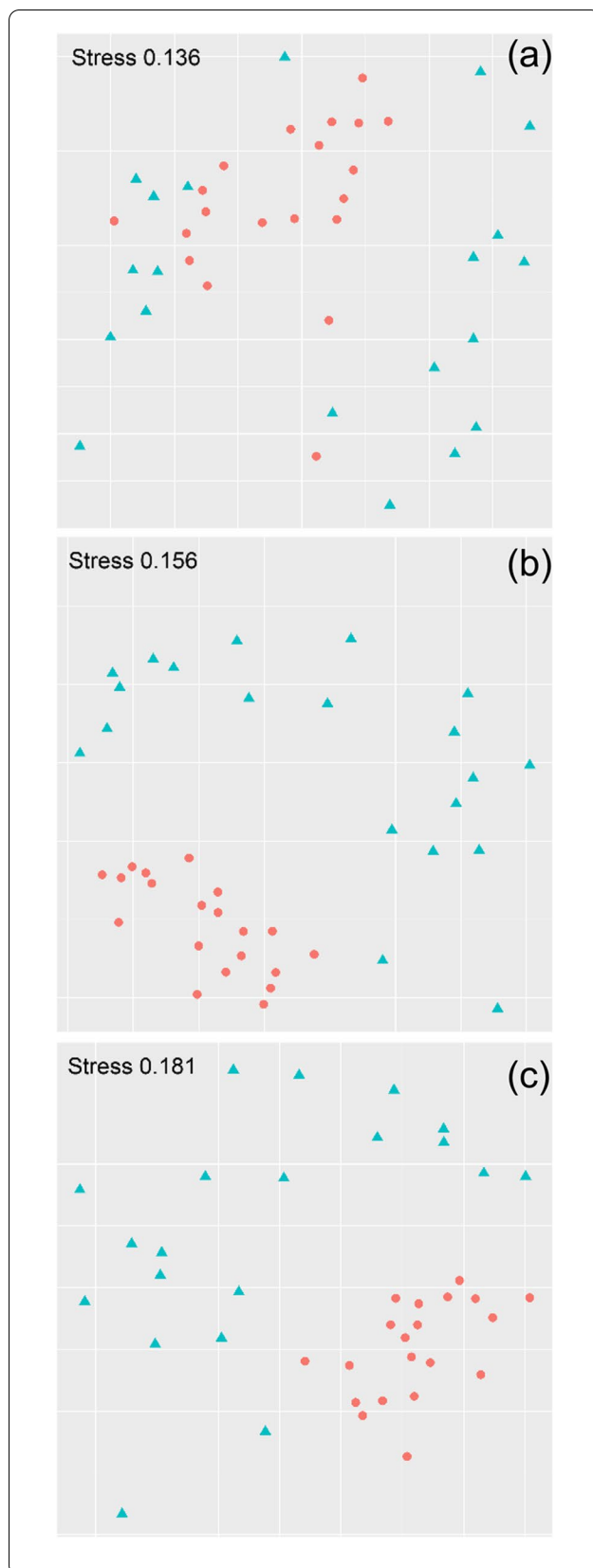


**Fig. 2** nMDS incorporating all the sampling sites in the surface (triangles) and deeper strata (circles). **a** Bray–Curtis measure without transformation, **b** Bray–Curtis measure with fourth root transformation, **c** Jaccard measure with data converted to presence-absence

in the deeper stratum). The homoscedasticity test for multivariate dispersion yielded significant heteroscedasticity between the two strata ( $p < 0.001$ ), therefore the PERMANOVA test was not performed, separating the zooplankton communities of the two strata in subsequent analyses. Greater community dissimilarity within the zooplankton community was observed between the two strata with the Bray–Curtis fourth root-transformed and the Jaccard presence-absence conversion (Fig. 2b, c).

The zooplankton data of the surface stratum indicate that the sample sites make up three groups with the Bray–Curtis measure without transformation, and two groups with this measure transformed to fourth root (Fig. 3a, b). The grouping obtained by the *K*-means method, for the data without transformation, yielded the highest silhouette values ( $s = 0.338$ ). These three homogeneous groups did not present multivariate overdispersion ( $p_{\text{homoced}} = 0.426$ , Table 1), but there were significant differences in their means ( $p_{\text{permanova}} = 0.001$ , Table 1). The grouping with the highest silhouette value ( $s = 0.316$ ) with the Bray–Curtis measure transformed to fourth root shows two groups that were also obtained with the *K*-means method. The groups were again homogenous and without multivariate overdispersion ( $p_{\text{homoced}} = 0.723$ , Table 1), but with a significant difference in their means ( $p_{\text{permanova}} = 0.001$ , Table 1). The dispersion was homogenous for the Jaccard measure, but no groupings with acceptable silhouette values were found (Fig. 3c). The dendrogram shown in Additional file 1 summarizes the dissimilarities among sampling sites in the surface stratum according to the groups obtained by the *K*-means method that yielded the highest cophenetic correlation. Site C12 is between two large groups, which in turn have two smaller groups, forming a total of five lesser groupings at an approximate dissimilarity of 50%.

With respect to the data for zooplankton in the deeper strata, groups with acceptable mean silhouette values ( $s = 0.33$ ) were only observed for the Bray–Curtis measure without transformation (Fig. 3d). The nMDS obtained with the Bray–Curtis fourth-root transformed and Jaccard did not yield clear groups and had

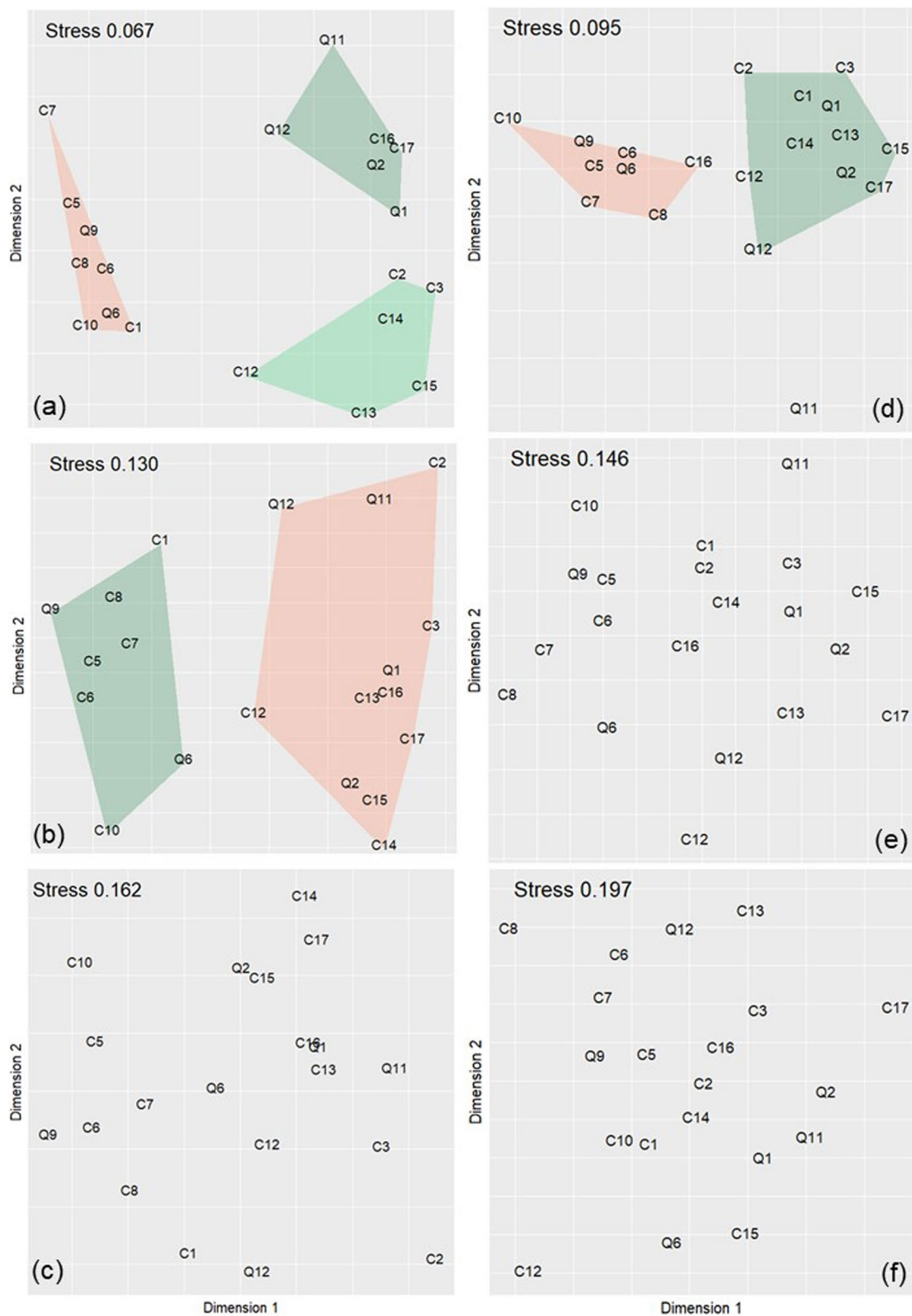


**Fig. 3** nMDS analysis for the surface (a-c) and deeper strata (d-f). **a, d** Bray–Curtis measure without transformation. **b, e** Bray–Curtis measure transformed to fourth root. **c, f** Jaccard measure converted to presence-absence. Color polygons in (a, b and d) indicate statistically different groups

**Table 1** Results of the silhouette coefficient, homoscedasticity and PERMANOVA tests for the zooplankton groupings from the surface and deeper strata identified in the nMDS analysis. The measure and data transformations are indicated. In bold  $p(\text{perm}) < 0.05$ 

Stratum	Measure	Groups	Silhouette	$F_{\text{hom}}$	$p_{\text{hom}}$	$F_{\text{perm}}$	$p_{\text{perm}}$
Surface	Bray–Curtis	3	0.338	0.897	0.426	10.377	<b>0.001</b>
Surface	Bray–Curtis (fourth root)	2	0.316	0.130	0.723	11.559	<b>0.001</b>
Deeper	Bray–Curtis	3	0.331	5.011	<b>0.019</b>	8.987	<b>0.001</b>
Deeper	Bray–Curtis (without Q11)	2	0.352	1.413	0.251	13.72	<b>0.001</b>

**Table 2** Results of the homoscedasticity tests and PERMANOVA to compare zooplankton in the two strata between sites near to and far from aquaculture centers. The resemblance measurements and data transformations are indicated

Stratum	Measure	$F_{\text{hom}}$	$p_{\text{hom}}$	$F_{\text{perm}}$	$p_{\text{perm}}$
Surface	Bray–Curtis	2.3368	0.1437	1.01350	0.373
Surface	Bray–Curtis (fourth root)	1.3279	0.2642	0.71549	0.597
Surface	Jaccard	0.4271	0.5217	0.60597	0.829
Deeper	Bray–Curtis	0.4001	0.5350	0.41552	0.919
Deeper	Bray–Curtis (fourth root)	0.0071	0.9340	0.72185	0.683
Deeper	Jaccard	0.1040	0.7508	0.96762	0.497

low silhouette values (Fig. 3e, f). The nMDS for this stratum indicates that Q11 was an outlier site (Fig. 3d), making a cluster by itself, as confirmed by the consensus dendrogram (see Additional file 1). With Q11 removed from the analysis, a good silhouette coefficient was obtained for the remaining sites ( $s = 0.352$ ), with better stress in the nMDS (0.072). The homoscedasticity test to assess multivariate overdispersion was not significant for these two groups ( $p_{\text{homoced}} = 0.251$ , Table 1), but there was a significant difference in their means ( $p_{\text{permanova}} = 0.001$ , Table 1). No significant differences were found between the zooplankton communities at sites near to and far from aquaculture farms, either at the surface or in deeper strata ( $p_{\text{permanova}} > 0.05$ , Table 2), considering the different dissimilarity measures and transformations. Multivariate overdispersion was not detected in either case (Table 2). Accordingly, two areas (northern and southern) were identified in Caucahué Channel with distinct zooplankton community characteristics based on the multivariate analyses. Discounting the outlier sites C1 and Q12 in the upper stratum and Q11, Q12 and C16 in the lower stratum, the north/south demarcation of the Caucahué Channel is represented by three and two groups in the surface stratum (Fig. 4a, b) and by two in the deeper stratum (Fig. 4c).

For the hydrographic/environmental variables of the water column, the distLM analysis indicated that sea temperature was a significant explanatory variable for the multivariate zooplankton groupings in both strata

(Table 3a, see also Fig. 5). The models that incorporated all environmental variables had  $R^2$  values between 39.69% and 55.82% (Table 3). For both strata, however, the best predictive model according to the AICc was the one that only incorporated the variable temperature (Table 3b–d). According to this model, during the zooplankton sampling day the northern section of the channel had higher average temperature than the southern section in both strata (see Additional file 2 and 3).

#### Univariate diversity and zooplankton spatial distribution

Average total abundance, species richness and dominance were higher in the southern section of the Caucahué Channel in both strata, while evenness and Shannon–Wiener diversity were higher in both strata of the northern section (Fig. 6). Forty-four taxa and/or morphotypes were identified in the surface stratum and 46 in the deeper stratum. Beta diversity, measured as the average dissimilarity between the northern and southern sections of the channel in the surface stratum, was 96.21% (SIMPER analysis); 91.20% of this dissimilarity was due to the relative abundance of the following taxa: *Metridia* sp. (copepod), Chaetognata Sp1, Hyperiididae sp1 (amphipod), Ostracoda Sp1, and *Pagurus* sp. (zoea) (Table 4). The average dissimilarity of the community structures between the deeper stratum of the northern and southern sections of the channel was 77.07% (SIMPER analysis); 91.09% was due to the relative abundance of the following taxa: *Metridia* sp., Chaetognata Sp1, Bryozoa

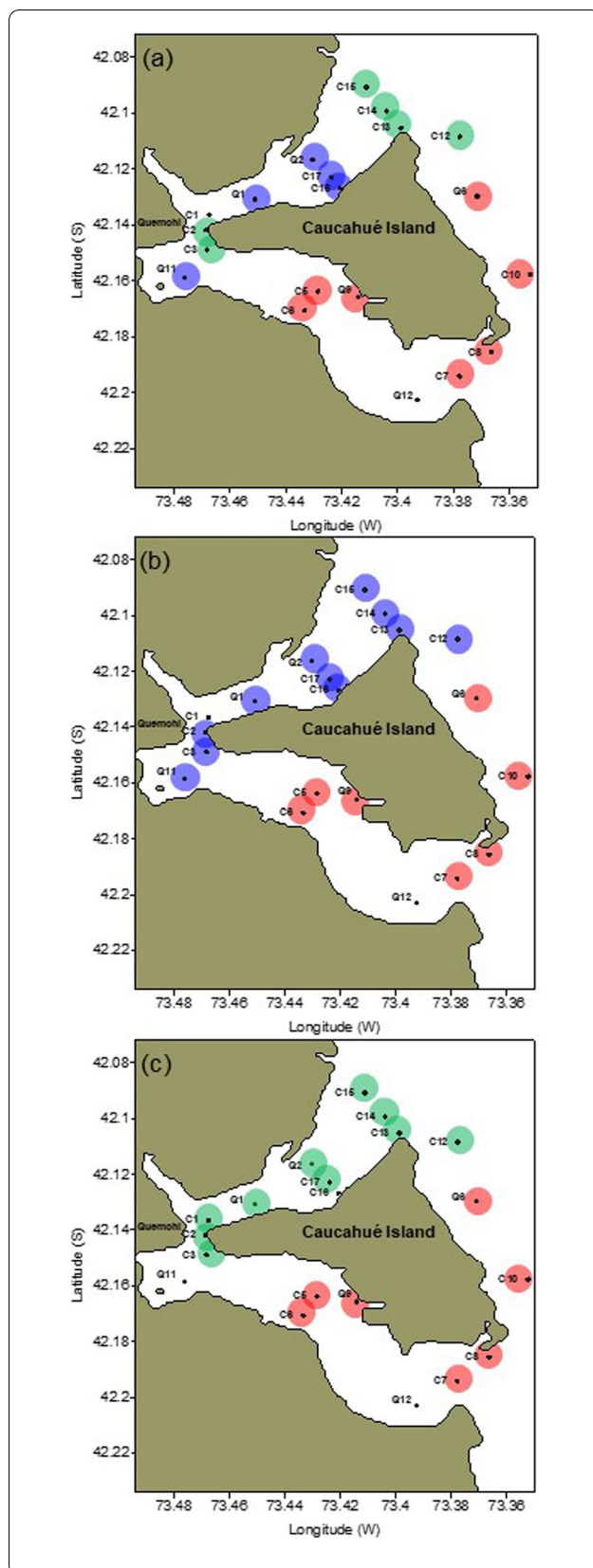


**Fig. 4** A spatial assignment of consensus for statistically significant zooplankton groupings for the surface (a, b) and deeper strata (c) in Caucahué Channel. The colors of the circumferences identify the different groups

larvae, *Acartia* sp. (copepod), *Paracalanus* sp. (copepod), Ostracoda Sp1, Syphonophore Sp1, *Calanoides patagoniensis* (copepod) and Isopoda Sp1. (Table 5). Tables 4 and 5 also show the species that contributed most to average community similarity in the two strata in the northern and southern sections of the Caucahué Channel. Total average abundances of meroplankton (0.22 ind 100 m<sup>-3</sup> northern surface stratum—2.33 ind 100 m<sup>-3</sup> southern surface stratum; 1.94 ind 100 m<sup>-3</sup> northern deeper stratum—4.50 ind 100 m<sup>-3</sup> southern deeper stratum) and holoplankton (2.30 ind 100 m<sup>-3</sup> northern surface stratum—63.3 ind 100 m<sup>-3</sup> southern surface stratum; 5.89 ind 100 m<sup>-3</sup> northern deeper stratum—23.81 ind 100 m<sup>-3</sup> southern deeper stratum) showed higher values in the southern section (Fig. 7a, b). Higher abundances of *Metridia* sp., Chaetognata Sp1, Hyperiididae sp1 (holoplankton); *Pagurus* sp., Caridea sp1 and *Callinasa* sp1 (meroplankton) were found in the southern section (Fig. 7c-h). Higher abundances were observed for five of these dominant taxa when sampling was carried out at dusk or night (Fig. 7c-h). No larval stages of the parasitic copepod *Caligus rogercreseeyi* were found during the sampling period in either stratum.

#### Chlorophyll and phaeopigments

Between 2 and 50 m depth the Chl-*a* average values were 0.30 ( $\pm 0.14$ ) and 0.39 ( $\pm 0.11$ ) mg m<sup>-3</sup> in the northern and southern sections, respectively, whereas the average phaeopigment concentrations were 0.18 ( $\pm 0.04$ ) and 0.19 ( $\pm 0.02$ ) mg m<sup>-3</sup> in the northern and southern sections, respectively. The southern section had higher mean values of Chl-*a* in all strata, whereas phaeopigments did not present a clear general pattern, and were slightly higher in the southern section in the surface and the deeper strata (see Additional file 4).

#### Hydrodynamics and hydrography

According to the local bathymetry of the Quemchi constriction, the total current dispersion tended to be oriented along the channel (north–south axis). Maximum currents reached near 80 cm s<sup>-1</sup> and were more intense southward (Fig. 8). Currents and sea level measurements spanned neap (3) and spring (2) tides, with maximum sea level amplitudes close

**Table 3** (a) Output of marginal tests for distLM analyses. In bold  $p < 0.05$ . (b-d) Output of best solutions for distLM analyses. The best result for each number of variables is shown. In bold the best model according to AICc criteria. 1 = Temperature, 2 = Salinity, 3 = Dissolved oxygen, 4 = pH, 5 = Redox potential

	Surface stratum, Bray–Curtis (not transformed)		Surface stratum, Bray–Curtis (fourth root)		Deeper stratum, Bray–Curtis (not transformed)	
<b>a) Marginal tests</b>	$R^2 = 39.69\%$		$R^2 = 41.66\%$		$R^2 = 55.82\%$	
<b>Variable</b>	<b>Pseudo-F</b>	<b>P</b>	<b>Pseudo-F</b>	<b>p</b>	<b>Pseudo-F</b>	<b>P</b>
Temperature (°C)	4.3821	<b>0.003</b>	5.9770	<b>&lt; 0.001</b>	9.5981	<b>0.001</b>
Salinity	1.4479	0.186	1.6571	0.129	0.3392	0.939
Dissolved oxygen (mL/L)	1.4824	0.174	1.1034	0.331	1.1887	0.268
pH	1.6074	0.136	1.2198	0.265	1.7748	0.111
Redox potential (mV)	2.2287	0.053	0.8652	0.487	0.5569	0.736
<b>b) Surface stratum, Bray–Curtis (not transformed)</b>	<b>AICc</b>	<b>R<sup>2</sup></b>	<b>RSS</b>	<b>N° Variables</b>	<b>Selections</b>	
	<b>162.33</b>	<b>0.19579</b>	<b>52,932</b>	<b>1</b>	<b>1</b>	
	162.08	0.30933	45,459	2	1;5	
	164.16	0.34559	43,072	3	1;4;5	
	166.82	0.37651	41,037	4	1;2;4;5	
	170.33	0.39686	39,698	5	All	
<b>c) Surface stratum, Bray–Curtis (fourth root)</b>	<b>147.78</b>	<b>0.24928</b>	<b>25,571</b>	<b>1</b>	<b>1</b>	
	149.08	0.30328	23,732	2	1;5	
	150.8	0.35165	22,084	3	1;2;5	
	153	0.39605	20,572	4	1;2;4;5	
	156.49	0.41663	19,871	5	All	
<b>d) Deeper stratum, Bray–Curtis (not transformed)</b>	<b>148.24</b>	<b>0.34778</b>	<b>26,175</b>	<b>1</b>	<b>1</b>	
	148.09	0.43703	22,593	2	1;4	
	148.66	0.50563	19,840	3	1;3;4	
	150.98	0.53683	18,588	4	1;3;4;5	
	154.2	0.55832	17,725	5	All	

to 3 m (Fig. 9a). The total current showed one single layer with intensifications due to spring tides (Fig. 9b). Tidal currents explained close to 86% and 77% of the north–south and east–west total current variability, respectively. The main tides were semidiurnal (M2 and S2), with mean amplitudes of 30 cm s<sup>-1</sup> and 12 cm s<sup>-1</sup>, respectively. The residual current fluctuated but showed a southward tendency (negative values) with predominance of a single circulation layer along the record (Fig. 9d), especially during neaps 01 and 03. Residual northward currents were less common and also covered the entire water column. Bottom temperatures fluctuated between 11 °C at the beginning of the record and 10.5 °C at the end (Fig. 9e). The mean vertical structure of these subtidal currents was southward throughout the water column, with values of approximately 6 cm s<sup>-1</sup> between 5 and 30 m depth.

The mean southward flow slowed at a depth of around 35 m, owing to an increase in the eastward component of about 5 cm s<sup>-1</sup> (Fig. 10). Considering a mean sectional area of 17,000 m<sup>2</sup> in Quemchi constriction, the southward net transport was 1037 m<sup>3</sup> s<sup>-1</sup>. The flood duration (in hours) during neaps 1 and 2 fluctuated between approximately 25 and 35 h. The duration of the ebb varied between about 50 h (neap 2) and 80 h (neap 1). During the spring tide, however, the flood and ebb duration was more similar, fluctuating between 80 and 90 h (See Additional file 5). In addition, during neap tides the average velocities during the ebbs were greater than the average velocities of the floods. The same was observed during the spring tides, but in this case the differences between the average velocities were lower (See Additional file 5). This asymmetry favored the southward flow observed. The

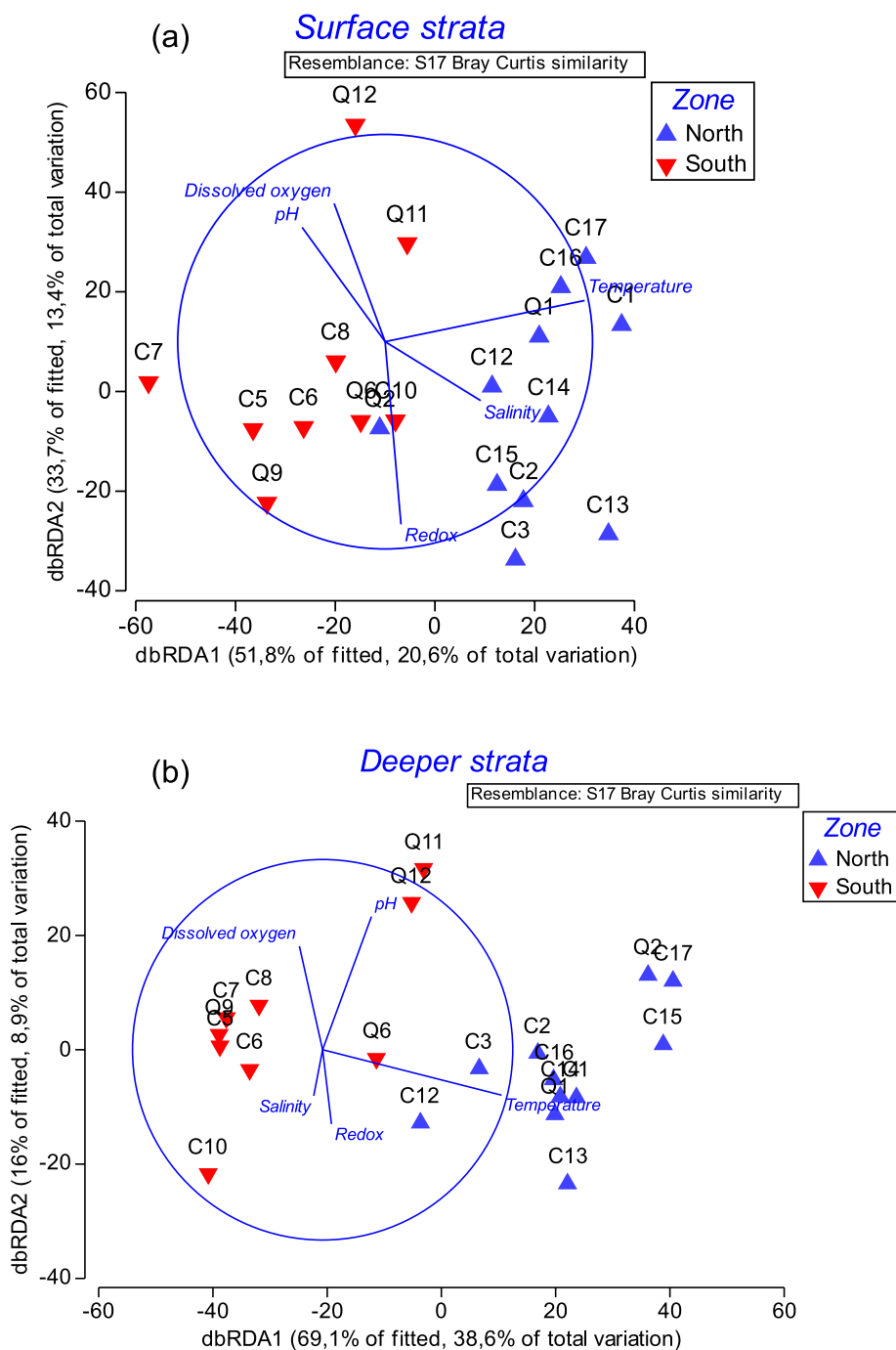
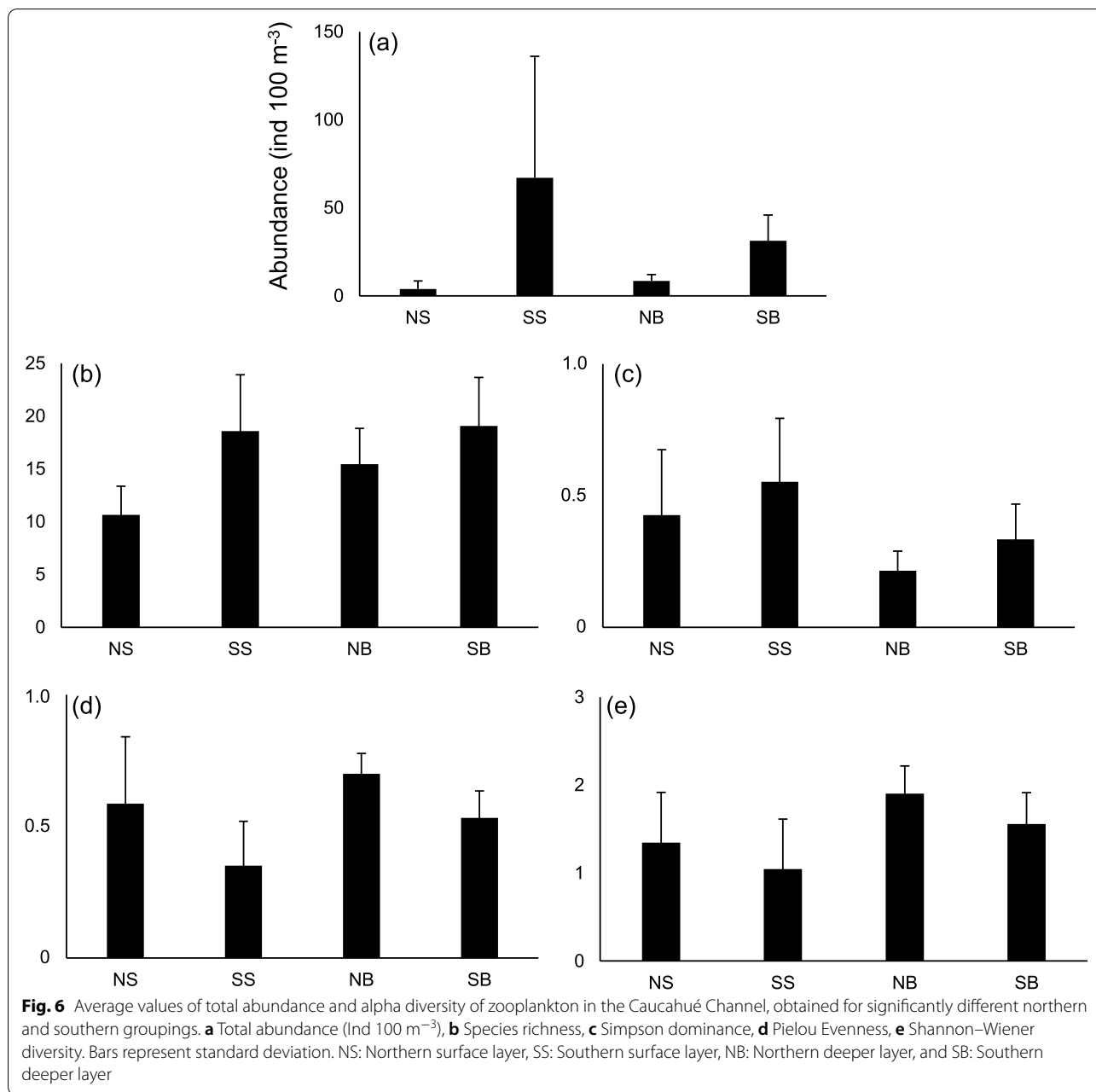


**Fig. 5** Graphical output of dbRDA analyses for (a) surface and (b) deeper strata. Multivariate arrangement of zooplankton community is shown in each plot. In both cases Bray–Curtis similarity measure without transformation is presented. Vectors of environmental variables are superimposed, showing Pearson correlation between scores of each dbRDA axis with each environmental variable

estimated values for the  $L_{adv}/L_{exc}$  ratio for 12 h in the neap ebb and flood phases were 2.9 and 0.8, respectively, while in spring ebb and flood phases they were 0.6 and 0.4, respectively. The estimated values for the

$L_{adv}/L_{exc}$  ratio for seven days in the neap ebb and flood phases were 40.6 and 11.0, whereas in the spring ebb and flood phases they were 8.6 and 5.7, respectively. These analyses indicate that for short periods (< 12 h),



the tidal excursion prevailed over the advective transport, favoring water retention. However, advective scales predominated for periods greater than seven days, favoring residual transport.

On June 19, the Caucahué channel showed a homogeneous vertical thermal structure with temperatures slightly warmer in the northern than in the southern section, ranging between 10.6 °C and 11 °C. Dissolved oxygen reached up to 7.5 mL L<sup>-1</sup> in mid-water (between 10 and 40 m depth); salinity was between 32.1 and 33.2, with the northern section being more

saline than the southern. As a result, the water column was slightly stratified (Fig. 11 a-d). The temperature was comparatively colder on June 30 than on the first cruise, showing a slight thermal inversion (Fig. 11 b). The distribution of dissolved oxygen and salinity was also lower (<5.2 mL L<sup>-1</sup> and <32.8) and more homogeneous in both cases compared to the first cruise (Fig. 11 f-g). As a result, the water column was lighter and more homogeneous than during the June 19 cruise (Fig. 11 f-g).

**Table 4** Results of the SIMPER analysis for the zooplankton community in the surface stratum of the Caucahué Channel. Av: Average, Ab: Abundance, Sim: Similarity, Dis: Dissimilarity, Cont %: Taxa percentage contribution, Cum %: Cumulative percentage taxa contribution

<b>Northern section group</b>						
<b>Average similarity: 28.94</b>						
<b>Taxa</b>	<b>Av. Ab</b>	<b>Av. Sim</b>	<b>Sim/SD</b>	<b>Cont %</b>	<b>Cum %</b>	
Hyperiididae Sp1	2.67	15.96	0.94	55.14	55.14	
Syphonophore Sp1	0.24	3.87	0.79	13.36	68.50	
<i>Calanus</i> sp.	0.16	2.58	0.63	8.92	77.42	
<i>Metridia</i> sp.	0.33	1.57	0.57	5.43	82.85	
<i>Stromateus stellatus</i> eggs	0.06	1.31	0.68	4.52	87.38	
Chaetognatha Sp1	0.10	1.20	0.68	4.16	91.54	
<b>Southern section group</b>						
<b>Average similarity: 51.47</b>						
<b>Taxa</b>	<b>Av. Ab</b>	<b>Av. Sim</b>	<b>Sim/SD</b>	<b>Cont %</b>	<b>Cum %</b>	
<i>Metridia</i> sp.	47.23	39.85	2.10	77.43	77.43	
Chaetognatha Sp1	11.98	6.53	0.97	12.68	90.11	
<b>Northern &amp; southern groups</b>						
<b>Average dissimilarity: 96.21</b>						
<b>Taxa</b>	<b>Northern Av. Ab</b>	<b>Southern Av. Ab</b>	<b>Av. Dis</b>	<b>Dis/SD</b>	<b>Cont %</b>	<b>Cum %</b>
<i>Metridia</i> sp.	0.33	47.23	62.08	3.64	64.53	64.53
Chaetognatha Sp1	0.10	11.98	14.23	1.47	14.80	79.32
Hyperiididae Sp1	2.67	0.44	5.21	0.59	5.41	84.74
Ostracoda Sp1	0.01	2.90	4.91	1.27	5.11	89.84
<i>Pagurus</i> sp. Zoea	0.00	0.80	1.30	0.66	1.35	91.20

## Discussion

There is currently great interest in gathering more information about the ecological and physical–chemical characteristics of receiving ecosystems of salmon and mussel farms in southern Chile, with the aim of minimizing their environmental impacts and thus making them more sustainable [6, 43, 44]. Despite the global importance of Patagonian ecosystems for salmon and mussel production, there have been few studies on the potential environmental impact of the sum of aquaculture centers located in a geographic unit, and fewer still that include salmon and mussel farms together [26, 44]. However, several studies have focused on the local effects (e.g. below or near the cages) of salmon farms on marine sediments, benthic macrofauna, phytoplankton, microbial communities and pesticides (e.g. [9, 45–49].).

### Spatial dissimilarities of zooplankton and environmental variables

Zooplankton measurements during a semidiurnal tidal cycle allowed a synoptic characterization of the most representative taxa within the channel, combined with

ebb and flood tidal currents and local hydrography. At this short time scale of observation, even considering the high intensity of tidal currents, the Caucahué Channel differentiates into northern and southern sections (Fig. 4). Both strata were differentiated by the multivariate analyses of the zooplankton communities, as well as by the univariate indicators of diversity and the total and relative abundance of the most representative species. In the southern section of the channel there was greater richness of species and greater total and relative abundance of dominant species, both holo- and mero-planktonic, resulting in lower evenness and diversity. For instance, higher abundances of copepods (*Metridia* Sp., and *Paracalanus* Sp.), chaetognaths, ostracods, bryozoan larvae and isopods were found in the southern section, favoring dissimilarities found between northern and southern sections of the channel, which were not found when the multivariate analysis was based only on the presence-absence of species. Free-living early stages of the copepods of *C. rogercreseeyi*, the most important salmonid ectoparasite in Patagonia [50], were not found in the Caucahué Channel, in the surface or deeper strata. It has been reported that

**Table 5** Results of the SIMPER analysis for the zooplankton community in the deeper stratum of the Caucahué Channel. Av: Average, Ab: Abundance, Sim: Similarity, Dis: Dissimilarity, Cont %: Taxa percentage contribution, Cum %: Cumulative percentage taxa contribution

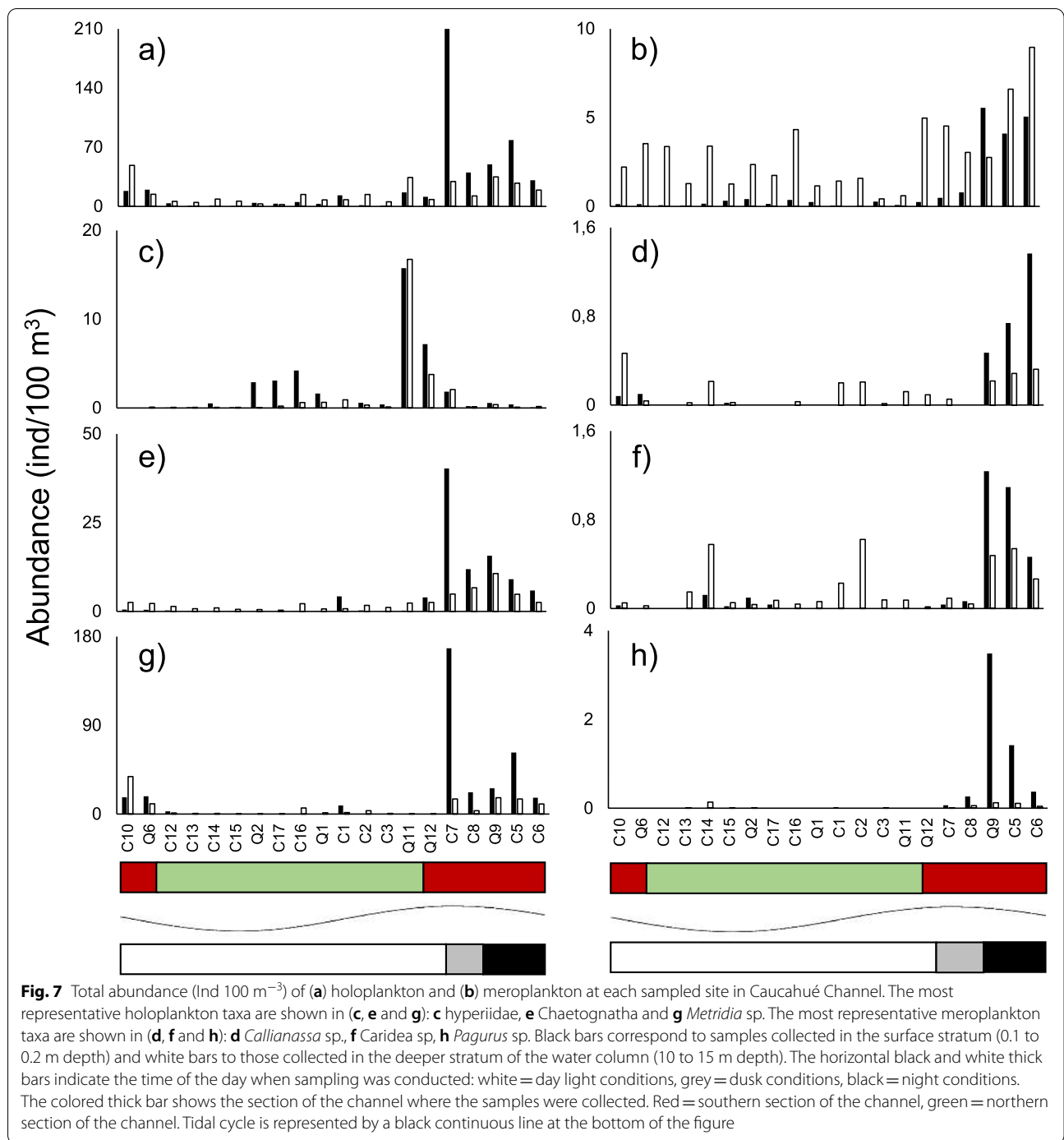
<b>Northern section group</b>						
<b>Average similarity: 49.81</b>						
<b>Taxa</b>	<b>Av. Ab</b>	<b>Av. Sim</b>	<b>Sim/SD</b>	<b>Cont %</b>	<b>Cum %</b>	
<i>Acartia</i> sp.	1.89	13.34	1.32	26.78	26.78	
Bryozoa larvae	1.44	11.09	1.29	22.26	49.04	
Chaetognatha Sp1	0.89	7.40	2.63	14.86	63.90	
<i>Metridia</i> sp.	1.05	5.75	1.18	11.54	75.44	
<i>Calanoides patagoniensis</i>	0.67	4.09	1.13	8.22	83.66	
Syphonophore Sp1	1.08	3.65	0.67	7.32	90.98	
<b>Southern section group</b>						
<b>Average similarity: 54.60</b>						
<b>Taxa</b>	<b>Av. Ab</b>	<b>Av. Sim</b>	<b>Sim/SD</b>	<b>Cont %</b>	<b>Cum %</b>	
<i>Metridia</i> sp.	15.66	28.58	2.34	52.33	52.33	
Chaetognatha Sp1	4.91	10.43	1.35	19.09	71.43	
Bryozoa larvae	3.97	8.12	1.62	14.87	86.30	
Ostracoda Sp1	1.19	2.28	1.35	4.18	90.48	
<b>Northern &amp; southern groups</b>						
<b>Average dissimilarity: 77.07</b>						
<b>Taxa</b>	<b>Northern Av. Ab</b>	<b>Southern Av. Ab</b>	<b>Av. Dis</b>	<b>Dis/SD</b>	<b>Cont %</b>	<b>Cum %</b>
<i>Metridia</i> sp.	1.05	15.66	33.06	2.06	42.89	42.89
Chaetognatha Sp1	0.89	4.91	11.34	1.33	14.72	57.61
Bryozoa larvae	1.44	3.97	7.44	1.21	9.65	67.26
<i>Acartia</i> sp.	1.89	0.24	4.90	1.11	6.35	73.61
<i>Paracalanus</i> sp.	0.17	1.48	3.26	0.87	4.23	77.84
Ostracoda Sp1	0.01	1.19	3.09	1.52	4.02	81.86
Syphonophore Sp1	1.08	0.03	2.84	0.75	3.69	85.54
<i>Calanoides patagoniensis</i>	0.67	0.63	2.18	1.00	2.83	88.38
Isopoda Sp1	0.08	0.92	2.09	0.91	2.71	91.09

*C. rogercresseyi* larval abundance in northern Patagonia was lower in winter in comparison to summer [21]. Because our sampling was carried out in winter, it was expected to find low abundance of the larval stages of this parasite in the water column.

It is interesting to note that no significant difference was found between zooplankton communities among sites close to and far from the six culture centers (14 sites far, 3 near salmon and 3 near mussel farms). This suggests that the spatial structure of the zooplankton community in the Caucahué Channel is mainly related to the north–south segregation related to the Quemchi constriction rather than the proximity to farms. Unfortunately there are no other studies carried out in Patagonia on the role of channel narrows in the spatial and temporal distribution of zooplankton. There is also no information in Patagonia on the potential effects of aquaculture farms (salmon and mussel) on survival and spatial–temporal distribution of holo- and

meroplankton. A study carried out in the Magdalen Islands (Gulf of Saint Lawrence, Canada) did not find differences in the plankton community comparing an area located a few dozen meters away from a bivalve aquaculture farm with another closer to the farm during a 6-month period [51]. Trotter et al. [51] suggested that their results can be explained by the fact that the bivalve farm was relatively small.

The differences in the zooplankton communities are also seen between strata, with a surface layer more heterogeneous and denser than the deeper layer (*i.e.* the surface stratum has a patchier spatial structure with higher abundance of zooplankton; See Figs. 6 and 7). Higher current velocities in the surface stratum could likely favor the generation of zooplankton patches. However, based on the information provided by the ADCP, no significant difference was found in the current between the surface (*i.e.* 1 m) and 15 m depth (Fig. 10, see also Additional file 6), which suggests a water column moving



in phase. Therefore, other factors could influence the smaller-scale spatial distribution in both sections of the Channel. For example, the total abundance of zooplankton and the dominant taxa in both strata could be related to the tidal cycle or the day-night cycle. Greater abundances of the most representative species of holo- and meroplankton were generally associated with the

transition from penumbra to darkness, which was coincidentally associated with the high tides (See Fig. 7). As a consequence, it is possible that vertical differences in total zooplankton, holo- and meroplankton, as well as in the most representative planktonic taxa in Caucahué Channel, could be related to vertical migration processes associated with tidal cycles or diurnal-nocturnal

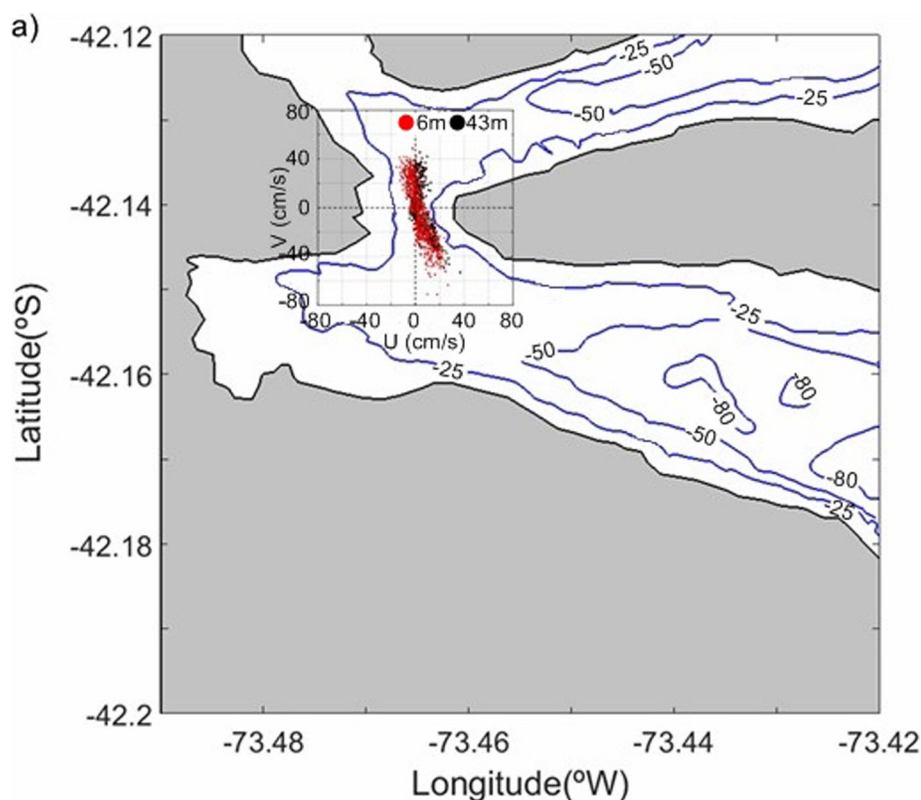


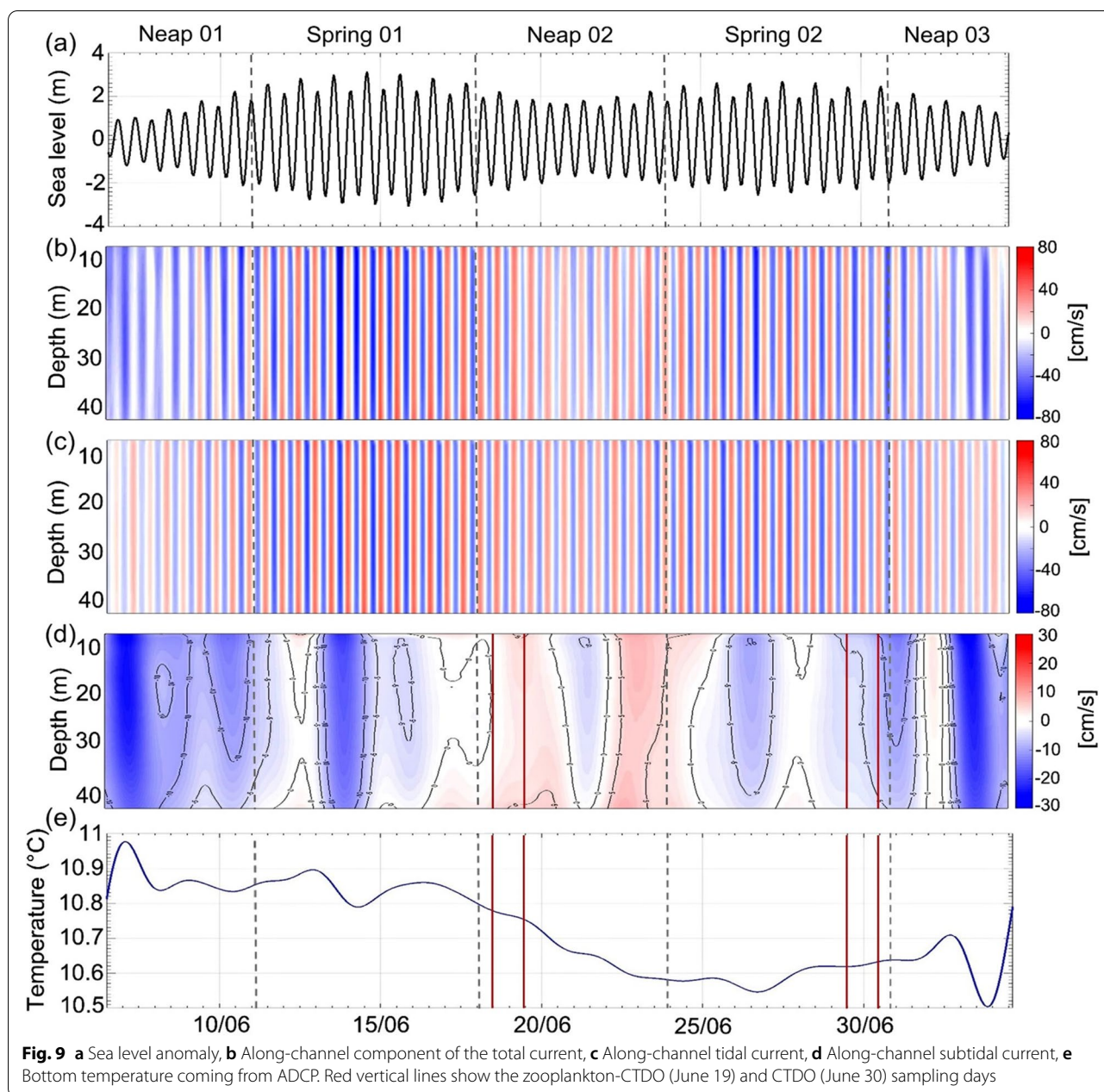
**Fig. 8** Dispersion diagram of the total current at 6 m (red dots) and 43 m (black dots) depths measured in the Quemchi constriction

displacements. In the Gulf of Ancud (inner sea of Chiloé), Castro et al. [52] also reported vertical short-term variations in mesozooplankton and ichthyoplankton abundance in a time period of 24 h associated with semi-diurnal tides.

In the short time scale of our study, the water column variables (temperature, salinity, dissolved oxygen, pH, and redox potential) together explained between 39.7% and 55.8% of the multivariate dissimilarities identified for the zooplankton communities of the two sections of the channel (see Table 3). Sea temperature correlated best with the biological differences observed between the two sections of the channel, with slightly lower temperatures in the southern section of the channel (See Figs. 5, and 11, Table 3 and Additional file 2 and 3). The southern section of the channel had slightly higher average values of Chl-*a* in the water column but with high spatial variability. The average values of dissolved oxygen and pH were also higher in the southern section, whereas salinity and redox potential were lower in this section of the Channel (See Figs. 5, and Additional file 2). These results suggest that even in this short time-sampling period, the measured water column variables (in a multivariate approach) were sufficiently

different to produce dissimilar environmental conditions between the two sections of Caucahué Channel. A study carried out in a similar period (June 21–24, 2014) [26] also found differences in environmental variables of the water column (temperature, salinity, dissolved oxygen, pH, among others, in a multivariate approach) between the two sections of the Caucahué Channel. It is important to note that our hydrographic sampling (June 19 and 30, 2014) was done in different transition phases from spring to neap tides. On June 19, subtidal currents tended to flow slightly northward, and on June 30 currents tended to flow with more intensity southward, probably favoring higher and lower hydrographic homogeneity, respectively (Fig. 9d and 9e).

Higher concentrations of ammonium and nitrate were found in the water column in the northern section of Caucahué Channel than in the southern section in the winter of 2014, whereas higher nitrite concentration was found in the southern section [49]. Another study conducted by our team in winter, 2019 (unpublished data) found higher concentrations of ammonium in the northern section and higher concentrations of nitrite, nitrate and phosphate in the southern section of the Caucahué Channel.



**Geomorphological constriction, hydrodynamics and zooplankton distribution**

The hydrodynamics of fjords and channels in Chilean Patagonia is influenced by local topographic features such as narrows and sills [53, 54]. One month of ADCP observations (June 6 to July 5, 2014) indicated a residual southward flow in the Caucahué constriction, with an average velocity of  $6.1 \text{ cm s}^{-1}$  and an average transport of  $1037 \text{ m}^3 \text{ s}^{-1}$  (Fig. 10). These current measurements corroborate those reported by Sobarzo

et al. [20] performed in 2011 in the southern section of the Caucahué Channel (April 19 to July 7, 2011). They indicated that the tidal excursion and residual flow determine the net transport, proposing that the origin of the residual southward flow was related to the non-linear effects of an oscillatory tidal current with bottom topography. This mechanism induced a tidal asymmetry clearly observable in the tidal currents. The southward direction of the residual flow in the

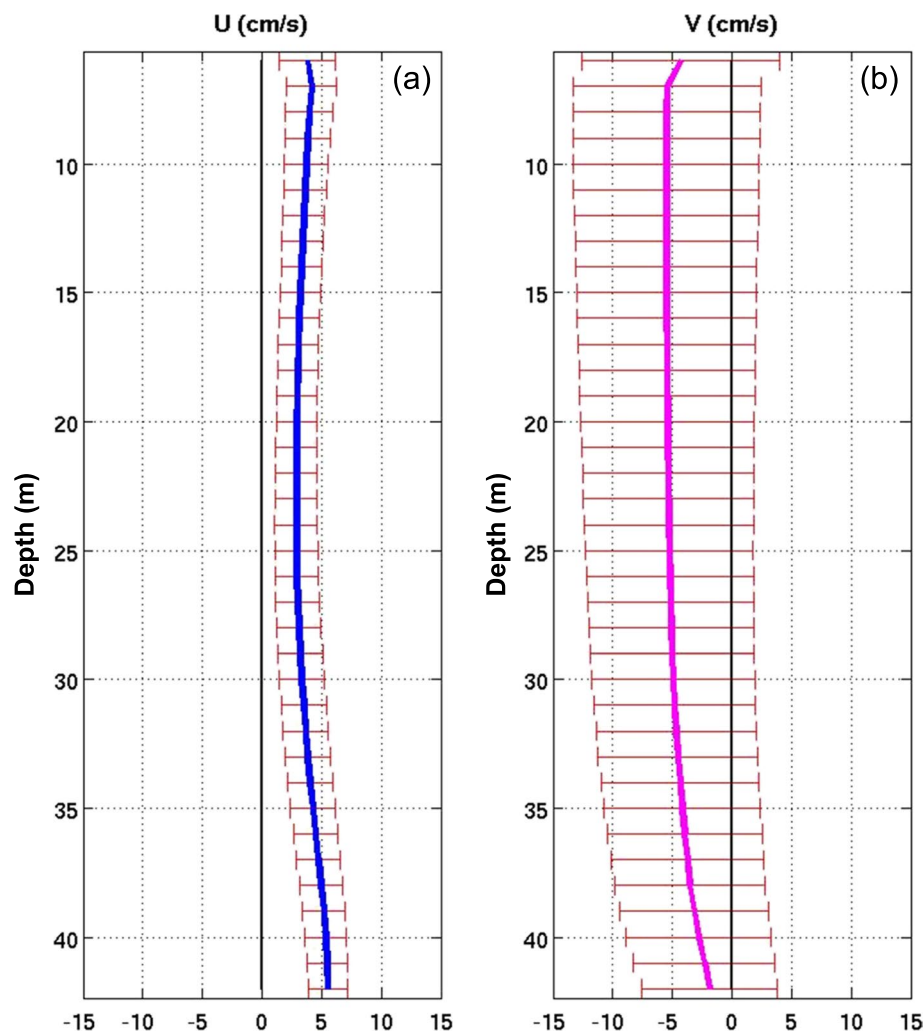
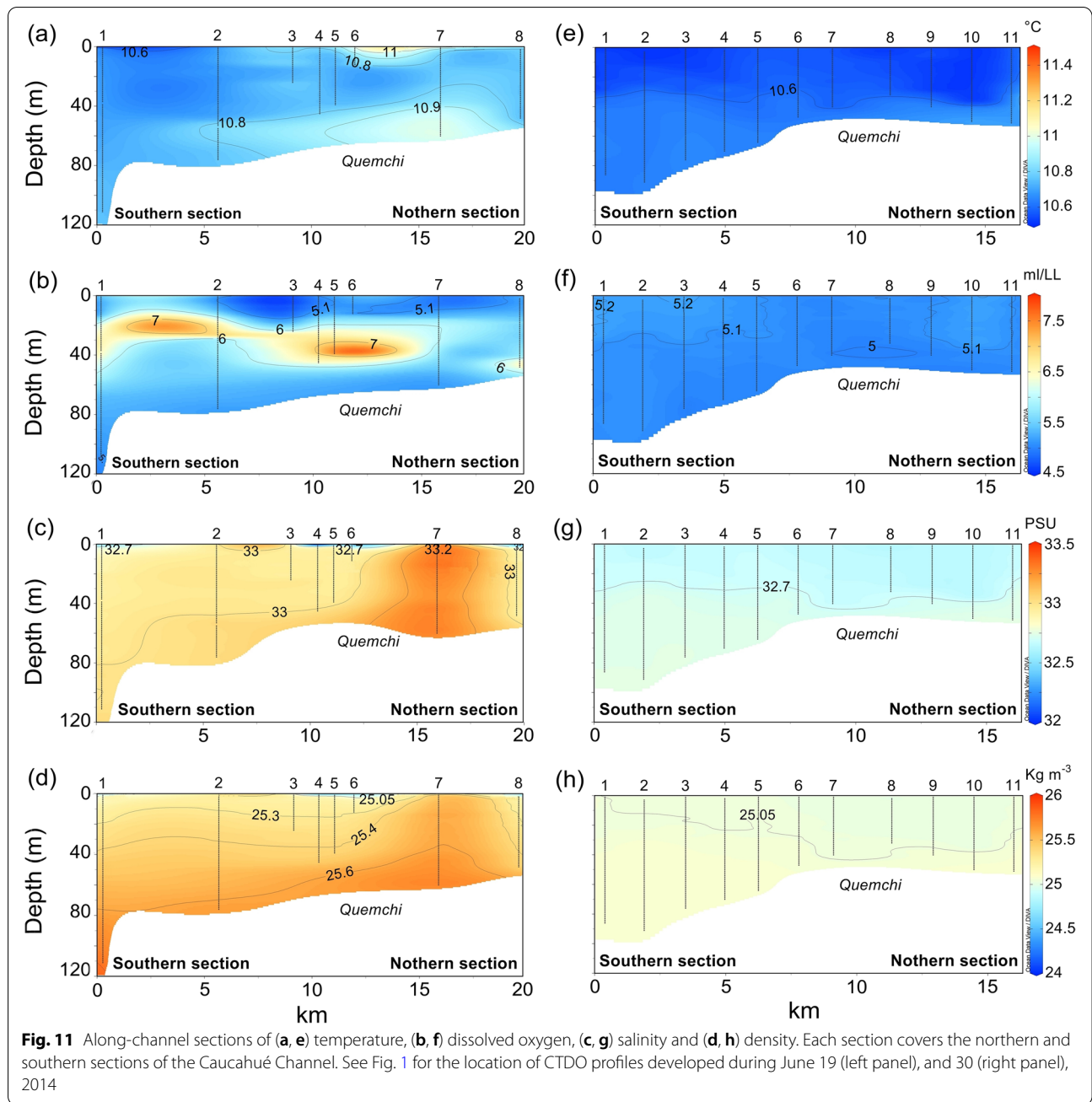


**Fig. 10** Mean vertical structure and variability of subtidal currents. **a** Cross-channel component, **b** Along-channel component. Horizontal lines in figures (a) and (b) represent one standard deviation

Quemchi constriction may explain in part why during the ISA virus outbreak in 2007–2009, only the salmon farms located in the southern section of the Channel had infected fish, and the disease did not spread to the northern section [55, 56].

The zooplankton sampling was performed in the spring/neap transition with at least 5–6 days of low southward transport (see Fig. 9d, and Additional file 6). In other words, the Quemchi constriction acted as a physical barrier between the sections of the channel during at least 5–6 days (spring tidal periods), promoting the biological and environmental differentiation observed on June 19. According to our hypothesis that the hydrodynamics of Caucahué Channel is forced by the geomorphological constriction, the fortnightly dynamics could favor retention mechanisms in each section of the channel in a time

scale of days, increasing or decreasing differentially in each channel section the abundance and concentrations of biotic and abiotic components of the water column (Fig. 12). The higher total abundance and zooplankton species richness in both depth strata of the southern section of the channel and dissimilarities in the zooplankton community and environmental variables suggest that the decrease in the residual flow produced by the geomorphological constriction in spring tidal periods could generate biological and chemical differences between the two sections of the channel in only a few days. These differences could be even larger in periods of high biological productivity like spring and summer, when spring tidal periods of 7 days can lead to major changes in primary productivity, occurrence of phytoplankton blooms and higher population growth of zooplankton species with high reproductive rates.



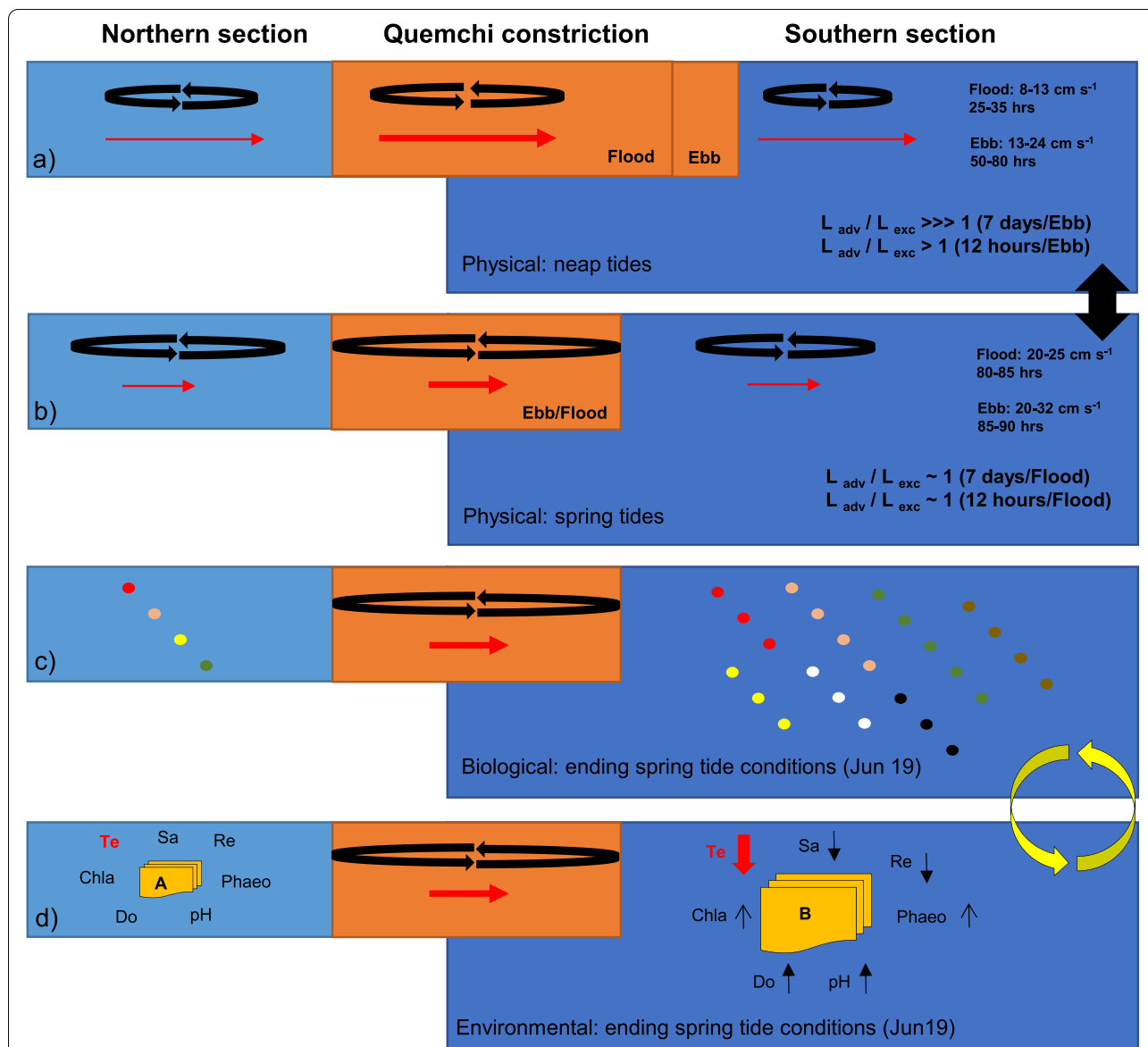


**Fig. 12** Conceptual diagram for Caucahué channel integrating the results obtained during the zooplankton sampling period (12 h, June 19). Black arrows = counterclockwise tidal excursion. Red arrows: southward residual flow. **a** and **b** show the ratios  $L_{adv}$  and  $L_{exc}$  estimated according to Sobarzo et al. (2018) [20], indicating the net southward transport between the sections of the channel and also the speed recorded for the ebb and flood phases in the neap and spring fortnightly periods estimated in this study. Color circles in **(c)** represent conceptually the different species of the zooplankton community and their relative abundances. Yellow arrows indicate the biological-environmental relationships in the water column. **d** shows the studied environmental variables in both sections of the Caucahué channel and how they differ on June 19, indicated by the direction of the arrow (see also DistLM analysis)

## Conclusions

The main conclusions of this investigation are: (i) At the time scale studied, clear dissimilarity in zooplankton composition were found between the two sections of Caucahué Channel; and (ii) the Quemchi geomorphological constriction and the asymmetrical southward residual flow could act as a physical barrier, favoring the spatial dissimilarities found in biotic and abiotic variables between the two sections of the channel.

## Abbreviations

HABs: Harmful algal blooms; ISA: Infectious Salmon Anemia; AMAs: Aquaculture Management Areas; ADCP: Acoustic Doppler Current Profiler.

## Supplementary Information

The online version contains supplementary material available at <https://doi.org/10.1186/s40693-022-00111-z>.

**Additional file 1.** Consensus dendrograms incorporating all sampling sites in (a) the surface and (b) deeper strata. Both estimations were made with the Bray-Curtis measure calculated without transformed data.

**Additional file 2.** Average values of environmental variables in the Caucahué Channel, obtained for northern and southern sections using a YSI multiprobe sensor. (a) Temperature, (b) Salinity, (c) Dissolved oxygen, (d) pH, (e) Redox potential. Bars represent standard deviation. NS: Northern surface layer, SS: Southern surface layer, NB: Northern deeper layer, and SB: Southern deeper layer.

**Additional file 3.** Vertical Profiles of temperature ( $^{\circ}\text{C}$ ), dissolved oxygen ( $\text{mL L}^{-1}$ ), salinity, and density ( $\text{Kg m}^{-3}$ ) obtained in Caucahué Channel during June 19 in similar sampling sites of zooplankton.

**Additional file 4.** Average values of chlorophyll-a (a, c) and phaeopigments (b, d) in the Caucahué Channel obtained for northern and southern sections. (a, b) correspond to average values of the integrated water column. (c, d) correspond to average values of the water column according to each depth stratum sampled. Bars represent standard deviation.

**Additional file 5.** (a) Number of hours with flood and ebb flows during the first two neaps periods, (b) Number of hours with flood and ebb flows during the two spring periods, (c) Along-channel mean velocities with flood and ebb during the first two neaps periods and (d) Along-channel mean velocities with flood and ebb during the two spring periods. All calculations were made using the total current. See also Methods section.

**Additional file 6.** Meridional current ( $v$ ,  $\text{cm s}^{-1}$ ) in Quemchi constriction, obtained from June 6 to July 4, 2014. This figure described currents at 5 and 15 m of depth. Black arrows show the sampling days of 19 and 30 of June.

## Acknowledgements

This research was funded by the Interdisciplinary Center for Aquaculture Research, INCAR (ANID; FONDAF 15110027). We wish to thank Alvaro Arana, Santiago Miranda, Sergio Pérez, Claudia Beltrán, Denise Recart, M. Cristina Krautz and Rodrigo Veas for their support in the fieldwork and sample analysis.

## Authors' contributions

EHM: Conceptualization, Methodology, Formal analysis, Investigation, Writing Original Draft. IB: Formal analysis. OV: Formal analysis. CI: Formal analysis. MS: Methodology, Writing—Review & Editing. RQ: Conceptualization, Methodology, Investigation, Writing—Review & Editing. All authors read and approved the final manuscript.

## Funding

This research was funded by the Interdisciplinary Center for Aquaculture Research, INCAR (FONDAF-ANID 15110027). The funders had no role in the study design, data collection, analysis, decision to publish or preparation of the manuscript.

## Availability of data and materials

The datasets used in the current study are available from the corresponding author on reasonable request.

## Declarations

### Ethics approval and consent to participate

Not applicable.

### Consent for publication

Not applicable.

### Competing interests

The authors have declared that no competing interests exist.

### Author details

<sup>1</sup>Interdisciplinary Center for Aquaculture Research (INCAR), Universidad de Concepción, Casilla 160-C, Concepción, Chile. <sup>2</sup>Departamento de Ecología, Facultad de Ciencias, Universidad Católica de La Santísima Concepción, Concepción, Chile. <sup>3</sup>Programa de Magíster en Estadística Aplicada, Departamento de Estadística, Universidad de Concepción, Concepción, Chile. <sup>4</sup>Departamento de Oceanografía, Facultad de Ciencias Naturales Y Oceanográficas, Universidad de Concepción, Concepción, Chile. <sup>5</sup>Programa de Doctorado en Oceanografía, Departamento de Oceanografía, Facultad de Ciencias Naturales Y Oceanográficas, Universidad de Concepción, Concepción, Chile.

Received: 18 March 2022 Accepted: 3 October 2022

Published online: 17 October 2022

## References

1. Aguilar-Manjarrez J, Soto D, Brummett R. Aquaculture zoning, site selection and area management under the ecosystem approach to aquaculture. Washington: Rome, FAO, and World Bank Group; 2017. p. 395 Full document. Report ACS113536.
2. FAO. El estado mundial de la pesca y la acuicultura 2020. La sostenibilidad en acción. Roma: Food and Agriculture Organization of the United Nations, Rome; 2020. p. 223. <https://doi.org/10.4060/ca9229es>.
3. SERNAPESCA. 2014. Anuario estadístico de pesca. Desembarques y acuicultura. <http://www.sernapesca.cl/>
4. Estay M, Chávez C. Local decisions and regulatory changes: the case of the Chilean aquaculture. *Lat Am J Aquat Res.* 2015;43:700–17.
5. Salgado H, Bailey J, Tiller R, Ellis J. Stakeholder perceptions of the impacts from salmon aquaculture in the Chilean Patagonia. *Ocean Coast Manage.* 2015;118:189–204.
6. Alvia A. Chile Case: The Spatial Planning of Marine Cage Farming (Salmon). In: Aguilar-Manjarrez J, Soto D, Brummett R, editors. Aquaculture zoning, site selection and area management under the ecosystem approach to aquaculture. Washington: Rome, FAO, and World Bank Group; 2017. p. 395 Full document, pp. 170–197. Report ACS113536.
7. Dresdner J, Estay M. Biosecurity Versus Profits: A Multiobjective Model for the Aquaculture Industry. *J World Aquacult Soc.* 2016;47:61–73.
8. Chávez C, Dresdner J, Figueroa Y, Quiroga M. Main issues and challenges for sustainable development of salmon farming in Chile: a socio-economic perspective. *Rev Aquacult.* 2019;11(2):403–21.
9. Soto D, Norambuena F. Evaluation of salmon farming effects on marine systems in the inner seas of southern Chile: a large-scale mensurative experiment. *J Appl Ichthyol.* 2004;20:493–501.
10. Buschmann AH, Riquelme VA, Hernández-González MC, Varela D, Jiménez JE, Henríquez LA, Vergara PA, Guíñez R, Filún L. A review of the impacts of salmonid farming on marine coastal ecosystems in the southeast Pacific. *ICES J Mar Sci.* 2006;63:1338–45.

11. Aguilera-Belmonte A, Inostroza I, Sáez Carrillo K, Franco JM, Riobó P, Gómez PI. The combined effect of salinity and temperature on the growth and toxin content of four Chilean strains of *Alexandrium catenella* (Whedon and Kofoid) Balech 1985 (Dinophyceae) isolated from an outbreak occurring in southern Chile in 2009. *Harmful Algae*. 2013;23:55–9.
12. Soto D, León-Muñoz J, Dresdner J, Luengo C, Tapia FJ, Garreaud R. Salmon farming vulnerability to climate change in southern Chile: understanding the biophysical, socioeconomic and governance links. *Rev Aquacult*. 2019;11(2):354–74.
13. Díaz PA, Molinet C, Seguel M, Díaz M, Labra G, Figueroa RI. Coupling planktonic and benthic shifts during a bloom of *Alexandrium catenella* in southern Chile: Implications for bloom dynamics and recurrence. *Harmful Algae*. 2014;40:9–22.
14. Soto D, Salazar FJ, Alfaro MA. Considerations for comparative evaluation of environmental costs of livestock and salmon farming in southern Chile. In: Bartley DM, Brugère C, Soto D, Gerber P, Harvey B, editors. Comparative assessment of the environmental costs of aquaculture and other food production sectors: methods for meaningful comparisons, pp. 121–136. Vancouver: FAO Fisheries Proceedings No. 10. Rome, FAO; 2007. p. 241 FAO/WFT Expert Workshop, 24–28 April 2006.
15. Asche F, Hansen H, Tveteras R, Tveteras S. The salmon disease crisis in Chile. *Mar Resour Econ*. 2009;24:405–11.
16. Tironi A, Marin VH, Campuzano FJ. A management tool for assessing aquaculture environmental impacts in Chilean Patagonian fjords: Integrating hydrodynamic and pellets dispersion models. *Environ Manage*. 2010;45:953–62.
17. Ibieta P, Tapia V, Venegas C, Hausdorf M, Takle H. Chilean salmon farming on the horizon of sustainability: review of the development of a highly intensive production, the ISA crisis and implemented actions to reconstruct a more sustainable aquaculture industry. In: Sladonja B, editors. *Aquaculture and the Environment - A Shared Destiny*. Rijeka: INTECH; 2011. pp. 215–46.
18. Hamilton-West C, Arriagada G, Yatabe T, Valdés P, Hervé-Claude LP, Urcey S. Epidemiological description of the sea lice (*Caligus rogercresseyi*) situation in southern Chile in August 2007. *Prev Vet Med*. 2012;104:341–5.
19. Corner RA, Aguilar-Manjarez J. Tools and Models for Aquaculture Zoning, Site Selection and Area Management. In: Aguilar-Manjarez J, Soto D, Brummett R, editors. *Aquaculture zoning, site selection and area management under the ecosystem approach to aquaculture*. Washington: Rome, FAO, and World Bank Group; 2017. Full document, pp. 95–145. Report ACS113536.
20. Sobarzo M, Bravo L, Iturra C, Troncoso A, Riquelme R, Campos P, Agurto C. Hydrodynamics of a channel occupied by the aquaculture industry in southern Chile: implications for connectivity between farms. *Aquacult Env Interac*. 2018;291:291–307.
21. Molinet C, Cáceres M, González MT, Carvajal J, Ascencio G, Díaz M, Díaz P, Castro MT, Codjambassis J. Population dynamic of early stages of *Caligus rogercresseyi* in an embayment used for intensive salmon farms in Chilean inland seas. *Aquaculture*. 2011;312:62–71.
22. Pearson T, Rosenberg R. Macrobenthic succession in relation to organic enrichment and pollution of the marine environments. *Oceanogr Mar Biol*. 1978;16:229–311.
23. Dauer DM. Biological criteria, environmental health and estuarine macrobenthic community structure. *Mar Pollut Bull*. 1993;26(5):249–57.
24. Borja A, Franco J, Pérez V. A marine biotic index to establish the ecological quality of soft-bottom benthos within European estuarine and coastal environments. *Mar Pollut Bull*. 2000;40:1100–14.
25. Borja A, Muxika I, Franco J. The application of a marine biotic index to different impact sources affecting soft-bottom benthic communities along European coasts. *Mar Pollut Bull*. 2003;46:835–45.
26. Hernández-Miranda E, Estrada R, Strange P, Veas R, Krautz MC, Quiñones RA. Macrofauna community patterns in a Chiloe Island channel used intensely for aquaculture: the ecological status of its benthic environment. *Rev Chil Hist Nat*. 2021;94:1–19. <https://doi.org/10.1186/s40693-021-00098-z>.
27. Bianchi F, Aciri F, Aubry FB, Berton A, Boldrin A, Camatti E, Cassin D, Comaschi A. Can plankton communities be considered as bio-indicators of water quality in the Lagoon of Venice? *Mar Pollut Bull*. 2003;46:964–71.
28. Webber M, Edwards-Myers E, Campbell C, Webber D. Phytoplankton and zooplankton as indicators of water quality in Discovery Bay, Jamaica *Hydrobiologia*. 2005;545:177–93.
29. Casé M, Leça EE, Leitão SN, Sant'Anna EE, Schwaborn R, Travassos de Moraes Junior A. Plankton community as an indicator of water quality in tropical shrimp culture ponds. *Mar Pollut Bull*. 2008;56:1343–52.
30. Niemi GJ, McDonald ME. Application of Ecological Indicators. *Annu Rev Ecol Syst*. 2004;35:89–111.
31. Beaugrand G. Monitoring pelagic ecosystems using plankton indicators. *ICES J Mar Sci*. 2005;62:333–8.
32. Racault M-F, Platt T, Sathyendranath S, Agirbas E, Martínez V, Brewin R. Plankton indicators and ocean observing systems: support to the marine ecosystem state assessment. *J Plankton Res*. 2014;36(3):621–9.
33. Krautz MC, Hernández-Miranda E, Veas R, Bocaz P, Riquelme P, Quiñones RA. An estimate of the percentage of non-predatory dead variability in coastal zooplankton of the southern Humboldt Current System. *Mar Environ Res*. 2017;132:103–16.
34. Holm-Hansen O, Riemann B. Chlorophyll-a determination: improvements in methodology. *Oikos*. 1978;30:438–47.
35. Pawłowicz R, Beardsley B, Lentz S. Classical tidal harmonic analysis including error estimates in MATLAB using T\_TIDE. *Comput Geosci*. 2002;28:929–37.
36. Anderson M. A new method for non-parametric multivariate analysis of variance. *Austral Ecol*. 2001;26:32–46.
37. Anderson M. PERMANOVA: a FORTRAN computer program for permutational multivariate analysis of variance. Department of Statistics: University of Auckland, New Zealand; 2005. p. 24.
38. Anderson MJ, Gorley RN, Clarke KR. PERMANOVA+ for PRIMER: guide to software and statistical methods. Plymouth: PRIMER-E; 2008.
39. Sokal R, Rohlf F. The Comparison of Dendrograms by Objective Methods. *Taxon*. 1962;11:33–40.
40. Rousseeuw PJ. Silhouettes: A graphical aid to the interpretation and validation of cluster analysis. *Journal of Computational and Applied Mathematics*, Volume 20. ISSN. 1987;53–65:0377–427.
41. Kauffman L, Rousseeuw PJ. Finding groups in data: An introduction to cluster analysis. New York: Wiley Interscience; 1990.
42. Clarke KR, Gorley RN. PRIMER v6: user manual/tutorial. PRIMER-E, Plymouth. 2006.
43. Buschmann AH, Cabello F, Young K, Carvajal J, Varela DA, Henríquez L. Salmon aquaculture and coastal ecosystem health in Chile: Analysis of regulations, environmental impacts and bioremediation systems. *Ocean Coast Manage*. 2009;52:243–9.
44. Quiñones RA, Fuentes M, Montes RM, Soto D, León-Muñoz J. Environmental issues in Chilean salmon farming: a review. *Rev Aquacult*. 2019;11(2):375–402.
45. Aranda CP, Valenzuela C, Matamala Y, Godoy FA, Aranda N. Sulphur-cycling bacteria and ciliated protozoans in a Beggiatoaceae mat covering organically enriched sediments beneath a salmon farm in a southern Chilean fjord. *Mar Pollut Bull*. 2015;100:270–8.
46. Urbina MA. Temporal variation on environmental variables and pollution indicators in marine sediments under sea Salmon farming cages in protected and exposed zones in the Chilean inland Southern Sea. *Sci Total Environ*. 2016;573:841–53.
47. Olsen LM, Hernández KL, Ardelan MV, Iriarte JL, Sánchez N, González HE, Tokle N, Olsen Y. Responses in the microbial food web to increased rates of nutrient supply in a southern Chilean fjord: possible implications of cage aquaculture. *Aquacult Env Interac*. 2014;6:11–27.
48. Olsen LM, Hernández KL, Ardelan MV, Iriarte JL, Bizzel KC, Olsen Y. Responses in bacterial community structure to waste nutrients from aquaculture: an in situ microcosm experiment in a Chilean fjord. *Aquacult Env Interac*. 2017;9:21–32.
49. Valdés-Castro V, Fernandez C. Effect of Three Pesticides Used in Salmon Farming on Ammonium Uptake in Central-Southern and Northern Patagonia. *Chile Front Mar Sci*. 2021;7:602002. <https://doi.org/10.3389/fmars.2020.602002>.
50. Gallardo-Escárate C, Arriagada G, Carrera G, Goncalves AT, Nuñez-Acuña G, Valenzuela-Miranda D, Valenzuela-Muñoz V. The race between host and sea lice in the Chilean salmon farming: a genomic approach. *Rev Aquacult*. 2019;11(2):325–39.
51. Trottet A, Roy S, Tamigneaux E, Lovejoy C, Tremblay R. Influence of suspended mussel farming on planktonic communities in Grande-Entrée Lagoon, Magdalen Islands (Québec, Canada). *Aquaculture*. 2008;276:91–102.

52. Castro LR, Cáceres MA, Silva N, Muñoz MI, León R, Landaeta MF, Soto-Mendoza S. Short-term variations in mesozooplankton, ichthyoplankton, and nutrients associated with semi-diurnal tides in a Patagonian Gulf. *Continental Shelf Res.* 2011;31:282–92.
53. Valle-Levinson A, Jara F, Molinet C, Soto D. Observations of intratidal variability of flows over a sill/contraction combination in a Chilean fjord. *J Geophys Res.* 2001;106:7051–64.
54. Cáceres M, Valle-Levinson A, Molinet C, Castillo M, Bello M. Lateral variability of flow over a sill in a channel of southern Chile. *Ocean Dyn.* 2006;56:352–9.
55. Mardones FO, Pérez AM, Valdes-Donoso P, Carpenter TE. Farm-level reproduction number during an epidemic of infectious salmon anemia virus in southern Chile in 2007–2009. *Prev Vet Med.* 2011;102:175–84.
56. Mardones FO, Pérez AM, Carpenter TE. Epidemiologic investigation of the re-emergence of infectious salmon anemia virus in Chile. *Dis Aquat Organ.* 2009;84:105–14.

### Publisher's Note

Springer Nature remains neutral with regard to jurisdictional claims in published maps and institutional affiliations.

Ready to submit your research? Choose BMC and benefit from:

- fast, convenient online submission
- thorough peer review by experienced researchers in your field
- rapid publication on acceptance
- support for research data, including large and complex data types
- gold Open Access which fosters wider collaboration and increased citations
- maximum visibility for your research: over 100M website views per year

At BMC, research is always in progress.

Learn more [biomedcentral.com/submissions](https://biomedcentral.com/submissions)

